

General Disclaimer

One or more of the Following Statements may affect this Document

- This document has been reproduced from the best copy furnished by the organizational source. It is being released in the interest of making available as much information as possible.
- This document may contain data, which exceeds the sheet parameters. It was furnished in this condition by the organizational source and is the best copy available.
- This document may contain tone-on-tone or color graphs, charts and/or pictures, which have been reproduced in black and white.
- This document is paginated as submitted by the original source.
- Portions of this document are not fully legible due to the historical nature of some of the material. However, it is the best reproduction available from the original submission.

University of California, San Diego
December 1978

Final Report for Period
December 17, 1974 - September 30, 1978
Contract NAS 8-31145
NASA Marshall Space Flight Center, AL.

THE PROBLEM OF LOW ENERGY PARTICLE MEASUREMENTS
IN THE MAGNETOSPHERE

Elden C. Whipple, Jr.
University of California, San Diego
La Jolla, California 92093

Abstract

The accurate measurement of low energy (< 100 eV) particle properties in the magnetosphere has been difficult, partly because of the low density of such particles, but more particularly because of spacecraft interference effects. Spacecraft-emitted photoelectrons and secondary electrons are generally present in the vicinity of the spacecraft and can be a source of confusion in the interpretation of measured electron fluxes. Spacecraft charging in the magnetosphere can cause large apparent shifts in the energy of the ambient plasma particles so that repelled particles are not counted, whereas attracted particles are detected with relatively large kinetic energies. Differential charging of spacecraft surfaces affects particle trajectories, distorting particle velocity distributions and creating additional potential barriers.

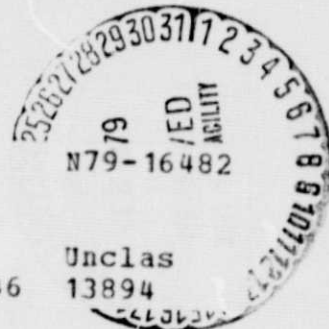
Some early examples of how these phenomena have affected particle measurements on an OGO spacecraft are presented. Data obtained with the UCSD particle detectors on ATS-6 are then presented showing how some of these difficulties have been partially overcome. Future measurements of low energy particles in the magnetosphere can be improved by:

- (1) improving the low energy resolution of detectors;
- (2) building electrostatically clean spacecraft; (2) controlling spacecraft potential; and (4) using auxiliary measurements, particularly wave data.

(NASA-CR-150907) THE PROBLEM OF LOW ENERGY
PARTICLE MEASUREMENTS IN THE MAGNETOSPHERE
Final Report, 17 Dec. 1974 - 30 Sep. 1978
(California Univ.) 48 p HC A03/MF A01

CSCI 04A G3/46

Unclas
13894



THE PROBLEM OF LOW ENERGY PARTICLE MEASUREMENTS
IN THE MAGNETOSPHERE

Elden C. Whipple, Jr.
University of California, San Diego
La Jolla, California 92093

1. INTRODUCTION

Low energy particle collection techniques such as ion mass spectrometers, ion traps and Langmuir probes have been used successfully for years in the ionosphere. However, it has been very difficult to obtain accurate measurements with these techniques of such important quantities as low energy ion and electron concentrations and temperatures in the magnetosphere. We use the term "low energy particles" for particles with energies below about 100 eV, with emphasis on the thermal particles at a few eV. The distinction between low and higher energy particles is more due to measurement techniques than it is to the physics of the magnetosphere. In this paper we describe the reasons for these measurement difficulties and give examples of some of the earlier attempts at making such measurements. Then we discuss how some of these difficulties have been partially overcome in the analysis and interpretation of ATS-6 data. Finally, we suggest how the measurement of low energy particle properties can be improved in the future.

The most significant feature of the magnetosphere that makes low energy particle measurements difficult is the low concentration of the particles.

At the plasmopause, which is generally taken to be the inner boundary of the magnetosphere, the charged particle density drops steeply from a few hundred (or perhaps a few thousand) particles per cm^3 to densities that may range from a few per cm^3 to perhaps as low as 10^{-2} per cm^3 in the magnetosphere proper. Since most particle detectors measure the current or flux that is collected, a very high sensitivity is required - typical currents are in the range from 10^{-10} to 10^{-14} amp or smaller for ions. This is well within the state of the art of even spacecraft instrumentation and is not a serious problem. The real problem is to distinguish these small currents from currents due to sources other than the magnetospheric plasma and to interpret the currents correctly in terms of the plasma properties.

Another effect of the low concentration of the particles, particularly when combined with the relatively high temperatures in the magnetosphere, is that the Debye length in the plasma is large - on the order of tens of meters. This is illustrated in Figure 1 where the Debye length is shown as a function of plasma density and temperature. The significance of this is that plasma perturbations caused by electric fields originating from a spacecraft will reach out relatively far into the plasma. Hence the currents collected by instruments will be affected significantly by such things as spacecraft charge or potentials on exposed spacecraft surfaces.

The predominant feature of the magnetosphere is the presence of energetic particles. There are relatively large fluxes at times of both energetic electrons and protons. These energetic particles can have a serious effect on the low energy particle measurements in two

ways. First, they constitute a source of low energy electrons by secondary emission from the spacecraft surfaces whenever a high energy particle strikes the spacecraft. Figures 2 and 3 show typical secondary emission yields for electron and proton impact. Second, collection of the high energy particles by the spacecraft is a source of spacecraft charge. If this is a dominant charging mechanism of the spacecraft, the spacecraft potential may rise to a value comparable to the energy of the particles. Even at much lower potentials, spacecraft charge is probably the most significant factor that makes low energy particle measurements difficult to interpret.

Another factor that contributes to both secondary electron currents and spacecraft charge is photoemission due to the shorter wavelengths of the solar radiation. Typical photoemission current densities are on the order of 3×10^{-9} amp/cm². In most of the magnetosphere this photoemission current density is larger than either the plasma ion or electron random current density.

Finally, as its name implies, the magnetosphere is characterized by the presence of the earth's magnetic field. The large scale motions of the plasma are controlled by the magnetic field. However, the magnitude of the field is small, On the scale of spacecraft dimensions, which is what is important as far as particle collection is concerned, the gyro-radii of both electrons and ions are large enough that the effect of the magnetic field is small, as is illustrated in Figure 4. On the other hand, the presence of the magnetic field together with the absence of particle collisions means that the properties of the plasma cannot be assumed to

be isotropic. The energetic particles have pitch angle distributions which may extend to the lower energy particles as well. If the velocity distributions are such that they can be characterized by temperatures, there may well be different temperatures for directions parallel to and transverse to the magnetic field. In addition, the bulk motion of the plasma may be distinguishable in the velocity distributions of the thermal particles. Any drift motion of the plasma will be closely related to the magnetic field direction as well as to the magnitude and direction of any electric fields that may be present.

2. EXAMPLES OF HOW MAGNETOSPHERIC PHENOMENA CAN AFFECT MEASUREMENTS

In this section some examples of early data obtained in the magnetosphere will be presented which illustrate some of the effects that have been mentioned. Figure 5 contains a series of low energy ion currents obtained within one hour by an ion trap on the OGO 1 satellite as it went out through the plasmopause. The saturation ion current dropped by more than three orders of magnitude during this time, until at 1920 UT it was approximately equal to the background current in the instrument caused by energetic particle fluxes. At higher altitudes, the thermal ion current could not be distinguished from these background currents.

Figures 6 and 7 illustrate the effects of solar radiation on measurements. In Figure 6 the satellite OGO 1 is in the earth's shadow so that there are no effects from the solar radiation. The ion current to the ion trap decreases as the retarding potential increases until only the background current due to energetic electrons remains. Five minutes later the satellite

has come out of the earth's shadow into sunlight. The magnitude of the ion current in Figure 7 is about the same as in Figure 6, but now the ion current cuts off at a much higher retarding potential, at about 14 volts rather than at 2 volts, indicating that the spacecraft potential has shifted by about 12 volts in a negative direction. In addition, in Figure 7 there is present a large peak in the current on the right-hand-side of the plot. The peak occurs during that part of the satellite spin period when the instrument is looking at the sun, and is a result of photoemission from both the collector and the grids of the instrument. The positive current at the center of the peak is due to those residual photoelectrons from the collector which were not suppressed by the suppressor grid. The negative currents in the wings of the peak are due to photoelectrons from the grids of the instrument which reach the collector to be registered as a negative current contribution.

The shift of the satellite potential by 12 volts in the negative direction as the spacecraft emerges from the earth's shadow into sunlight is in this instance not due to photoemission, but to the action of the large solar cell arrays. The arrays were connected to the positive terminals of the spacecraft batteries through a circuit which by-passed the batteries if the cells were not being charged (i.e., in darkness) so that the arrays were essentially at the spacecraft "ground" potential. In the sunlight the arrays were at the battery potential of about +28 volts with the result that the arrays acted as large attractive probes for collecting electrons from the surrounding thermal plasma, driving the spacecraft potential much more negative than it would have been otherwise.

The background current in Figure 6 due to energetic electrons illustrates the anisotropy in the particle velocity distributions that is frequently

present in the magnetosphere. In this case, the electrons have a pitch angle distribution such that the peak current is collected when the instrument axis is perpendicular to the local magnetic field. This occurs twice during one rotation of the spacecraft with the result that the background current modulation has a period twice that of the spacecraft spin.

Figures 8 and 9 illustrate the fact that secondary emission of electrons caused by energetic particle impact can be significant. During the time that the data in Figure 8 was obtained, the ion trap on OGO 1 was in a mode of operation designed for looking at thermal ions. One of the grids in the instrument was at -30 volts to keep thermal electrons with energies less than 30 eV from being collected. The background current due to energetic particles is 6×10^{-12} amp. In Figure 9 during an electron mode of operation designed for looking at the thermal electrons there is present a grid biased at +20 volts to keep out the thermal ions. Consequently, during the times that the data in the right-hand portion of Figure 8 and the data in the left-hand portion of Figure 9 were obtained, the instrument of the collector is equally accessible to energetic particles. Yet in Figure 9 the background current has a different magnitude and even a different polarity from that in Figure 8. The difference in the background currents in the two figures, since the thermal particles of both polarities with energies less than 30 eV are being kept from the collector, must be caused by secondary electrons produced in the sensor. By comparing the magnitude and polarity of the two background currents and using the known geometry of the grids and collector in the instrument it is possible to infer approximate values for the flux of energetic particles and the secondary emission yield (Whipple et al, 1968). For the data in Figures 8

and 9 the background currents are caused by a flux of approximately 3×10^6 protons/cm²-sec-ster with a yield on the order of two electrons emitted for every incident ion.

The change in the ion current cut-off potential between Figures 6 and 7 was taken as a measure of the change in satellite potential as the spacecraft went from darkness into sunlight. In Figure 10 the ion cut-off potential is plotted as a function of spacecraft position as the satellite goes to higher L-values in the magnetosphere. The spacecraft is in sunlight during this period so that at lower L-values where the thermal plasma density is relatively high, the solar arrays draw in a large number of electrons and drive the spacecraft to a relatively high negative potential. As the thermal plasma density decreases at larger L-values, fewer electrons are collected by the arrays and photoemission becomes a more important charging mechanism. As a result, the spacecraft potential becomes progressively less negative at the higher altitudes, and the ion cut-off potential occurs at lower potentials.

If it were not for the effect of the solar arrays, one would expect spacecraft potentials to become positive in the magnetosphere because of the dominant charging mechanism of photoemission. In contrast, expected spacecraft potentials in the ionosphere are on the order of a few tenths of a volt negative, corresponding to the equivalent electron temperature. These expectations are illustrated in Table 1 where a number of measured satellite potentials are given. Most of the satellites in near-earth orbit acquired potentials of a few tenths of a volt negative, with the exception of those satellites that had either long antennas or surfaces where electric fields were exposed to the plasma. All of the positive

potentials in Table 1 were obtained on satellites with orbits that took them well into the magnetosphere or into interplanetary space.

Charging currents due to fluxes of energetic particles are generally smaller than photoemission currents and would not affect spacecraft potentials appreciably if the spacecraft were in sunlight. However, magnetic storms can increase the fluxes of energetic particles and affect satellite potentials. DeForest (1972) measured a potential as large as 10^4 volts negative on ATS-5 during simultaneous magnetic storm and eclipse conditions. Figure 11 which is taken from DeForest's paper shows the change in the energy spectrum of both the energetic ions and electrons as the spacecraft goes from sunlight into eclipse. The energy of the protons increases while the energy of the electrons decreases, both by an equal amount of about 4.2 keV. His explanation is that the spacecraft has charged to a potential of -4.2 keV in the earth's shadow as a result of the increase in energetic particle fluxes and decrease in the thermal plasma density occasioned by a simultaneous magnetic sub-storm in the magnetosphere. If energetic particle fluxes are the dominant charging mechanism one would expect spacecraft potentials to be on the order of the particle energy. Frank (1972) has reported fluctuations of several hundred volts in particle energies measured with an instrument on IMP-6 which he attributes to spacecraft potential fluctuations. The fluctuations are most severe in low density regions of the magnetosphere such as the high-latitude magnetotail, and appear to be caused by an interaction between some of the spacecraft instrumentation and the plasma. Scarf (1972) has suggested that there is evidence from some satellites in the magnetosphere that differential charging has occurred on different insulated portions of

the spacecraft such that electric fields as large as kilovolts/meter occur between different portions of the spacecraft.

It is clear from the preceding discussion that there are a number of significant effects that must be taken into account in the interpretation of low energy particle data in the magnetosphere. On the other hand, these effects are for the most part well-understood theoretically and in addition can often be distinguished experimentally in the data. The real difficulty is to take them into account computationally with sufficient accuracy that the properties of the low energy plasma can be extracted reliably from the data. For example, spacecraft potential can usually be measured by instruments on the spacecraft and can be explained quite well in terms of the important charging mechanisms. The difficulty for low energy particle data comes in attempting to compute the effect of the spacecraft potential on the collected particles, since this requires a model of the spacecraft sheath and its effect on the particle orbits. The physical mechanisms of photoemission and secondary emission by energetic particle impact are well-understood theoretically (with some uncertainty for the yields) and the phenomena can usually be recognized experimentally in the data. The difficulty in taking them into account in data interpretation is again the computational problem of knowing how many secondary electrons reach the instrument so that the data can be corrected.

There have been few attempts at a self-consistent interpretation of both ion and electron data simultaneously obtained from particle instruments

on the same spacecraft in the magnetosphere. Such an analysis should yield equal ion and electron concentrations and hence constitute a test of the validity of the measurement and of the data analysis. One successful attempt used an assumed spherically symmetric Debye potential to assess the effect of spacecraft potential on the measured particle currents (Whipple et al, 1974). Ion and electron concentrations were both determined to be in the range from 1 to 3 per cm^3 .

It has also been possible to obtain a consistent interpretation of ion and electron data in the solar wind (Whipple and Parker, 1969). The task is admittedly easier in this region of space because of the relatively high energy of the ions in the solar wind. However, in the interpretation of the electron currents to the retarding potential analyzer on IMP 2 it was necessary to distinguish the plasma electron contributions from photoelectrons and secondary electrons, both of which yielded larger currents than the plasma electrons as shown in Figure 12. It was also necessary to take into account the effect of the satellite potential of +10 volts in enhancing the plasma electron current. Although the ion and electron measurements were not simultaneous, the agreement in the concentrations was excellent. A value of 4 cm^{-3} was obtained for the ion concentration and four hours later a value of 4.8 cm^{-3} was obtained for the electron concentration.

3. THE EFFECT OF ATS-6 CHARGING ON LOW ENERGY PARTICLE MEASUREMENTS

The ATS-6 satellite was launched on May 29, 1974 into a synchronous orbit where it was stationed at 94° W longitude, with an orbital inclination

of 1.8° . The spacecraft is fixed in orientation with respect to the earth and the large 10 m diameter parabolic reflector always points downward toward the earth (Figure 13). The UCSD experiment consists of five particle detectors mounted on the environmental measurement experiment module, a 1 m cube behind the center of the reflector (away from the earth).

The first four UCSD detectors consist of two pairs which rotate in direction. The fifth is a fixed detector of ions. Each pair consists of one detector for ions and one for electrons which rotate together through 220° in about 2.6 min, the first pair in a plane displaced 13° from the north-south plane, and the second pair in a plane displaced similarly from the east-west plane. Each detector is differential in both energy and angle: there are 64 energy steps spaced logarithmically from about 1 eV to 81 keV, and the energy resolution $\Delta E/E$ at each step is approximately 20%. The experiment has been described in more detail elsewhere (Mauk and McIlwain, 1975).

Detectors like the UCSD instrument which are differential in angle and energy have a distinct advantage over collection experiments of the kind described earlier. Collection experiments like Langmuir probes or retarding potential analyzers integrate over a large range of energy and angle of incidence for the incoming particles. Consequently, a great deal of the interpretation effort goes into determining the range of integration in velocity space, so that the plasma properties can be inferred accurately. The limits of integration are strongly dependent on the spacecraft potential but they can only be inferred indirectly from the data obtained with collection-type instruments. On the other hand, the data from differential instruments is directly related to the

particle velocity distribution function. Moreover, the allowed regions in velocity space over which particles from the plasma can reach the detector are usually apparent from the data itself. Consequently, it is more straightforward in general to infer the ambient plasma properties from the measurements. However, there are still problems in the interpretation of data from differential measurements. In this section we will describe some of these problems, as seen in data from the ATS-6 spacecraft.

Figure 14 displays a spectrogram which illustrates many of the typical effects of spacecraft charging on particle measurements. The spectrogram format has energy on the vertical scale and time along the horizontal axis. The count rate of the detectors as a function of energy and time is indicated by the gray scale, with white indicating a high count rate, and dark a smaller or zero count rate. The response of the north-south electron detector is given in the top half of the spectrogram, and the response of the north-south ion detector in the bottom half. Note that the energy scale, which is logarithmic, increases toward the bottom for ions.

At approximately 20:57 the spacecraft entered the earth's shadow, and the potential of the spacecraft which had been slightly positive in sunlight became slightly negative due to the disappearance of photoemission. As a result, low energy ions which had been kept away from the spacecraft by the repulsive positive potential, were now able to reach the spacecraft as shown by the bright band at low positive ion energies. Simultaneously, the bright band of low energy electrons disappears. As is discussed later, this band of electrons appears to be photoelectrons.

At about 21:22 there is a sudden "injection" of hot plasma into this region of the magnetosphere, and as a result the spacecraft charges to a negative potential of several kilovolts. This is indicated by the absence of ions below an energy threshold equivalent to the spacecraft potential. At this threshold energy, the count rate for the ions jumps abruptly to a very high value. This is caused by the acceleration of ambient low energy ions to a kinetic energy approximately equivalent to the potential of the spacecraft. As a result, most of the low energy ambient ions which reach the particle detector are collected in the first energy channel available above the spacecraft potential. (The thin dark band along this transition level is caused by the overflow of the spectrogram gray scale to the next level.)

This acceleration of low energy ions by the attractive potential on the spacecraft makes it difficult to infer accurately the density and temperature of these ions. Whenever the magnitude of the spacecraft potential is large compared to the thermal energy of the ions, most of the ions fall into a single energy channel of the detector because of the fact that the width of each channel increases proportionately to the energy itself ($\Delta E \approx 0.2 E$). The amplitude of this "charging spike" in the ion count rate depends sensitively on the exact spacecraft potential and on the shape of the collection efficiency curve of the detector within an energy channel.

At about 22:02 the spacecraft leaves eclipse conditions, and the potential of the spacecraft returns to about 50 volts negative. The threshold energy for the ions drops to this value. Also, there is an abrupt change at this time in the counting rate for the electrons. This is caused by the decreased repulsion of the spacecraft to the ambient electrons. Electrons with ambient energies below 3000 eV in eclipse could not reach the spacecraft, but now electrons with energies above about 50 eV are able

to penetrate to the spacecraft. The distribution functions and hence the count rates for these lower energy electrons are much higher than for the more energetic electrons, and consequently the spectrogram appears much brighter after eclipse.

The charging effects described so far are caused by the net charge on the spacecraft and the attraction or repulsion of this charge on the ambient plasma particles. Another important phenomenon which affects particle measurements is differential charging of the spacecraft where different portions of the spacecraft external surfaces may be charged to different potentials. This can occur on dielectric surfaces such as the glass cover slides of solar cells or on thermal blankets which are generally made of insulating material. Or conducting portions of the spacecraft surfaces may be electrically isolated from each other by insulation so that each such portion may come to a different equilibrium potential.

The presence of differential charging can have several consequences. First, there will be large electric fields present between the differentially charged regions. As a result, there can be electrical discharges between the regions or across intervening material with consequent material damage. Such discharges are thought to be responsible for many spacecraft anomalies (McPherson et al, 1976). Second, differential charging can result in the presence of a potential barrier around the spacecraft. This effect is illustrated in Figure 15, taken from some work by Mandell et al (1978). They have calculated the potential distribution about a dielectric "sphere" (actually an octagon) where one side is illuminated by the sun, and the other side is shadowed. The shaded side is at a potential of about -150 V whereas the sunlit side is at about -15 V. The equipotentials from the more negative shaded side curve around on the sunlit side to form a potential barrier at approximately -25 V. Photoelectrons from the sunlit side of the spacecraft cannot escape to the ambient plasma unless their kinetic

energy is sufficiently large to overcome the barrier height -- a differential of about 10 V, in spite of the fact that the spacecraft is negative with respect to the ambient plasma. The potential barrier also serves to keep ambient plasma electron with energies less than the barrier height of 25 eV from reaching the sunlit side of the spacecraft. This figure is for a non-equilibrium state during the charging process, 22.5 sec after the charging event started. The final equilibrium potential configuration had a barrier potential about five volts more negative than the sunlit side of the spacecraft.

A third effect of differential charging is that portions of the spacecraft surface which are more negative than the rest of the spacecraft can emit photoelectrons or secondary electrons which are then accelerated by the differential potential to other parts of the spacecraft. When these electrons enter a particle detector they are observed as sharp spikes in electron count rate at particular energies and for particular directions. These spikes can be considered to be "precursors" to discharges.

The presence of a potential barrier in the vicinity of the ATS-6 spacecraft has been previously inferred from the low energy electron data (Whipple, 1976). There is almost always a peak in the electron counting rate at an energy from 4 to 10 eV. It was shown from the inferred electron densities corresponding to this peak, as well as from the corresponding distribution functions and the behavior of the counting rate versus angle, that these electrons must be photoelectrons or secondary electrons originating at the spacecraft. Since these electrons were observed coming in at angles directly normal to the spacecraft surface, there must be a potential barrier in the sheath about the spacecraft which reflects the electrons and keeps them from escaping. It was inferred that differential

charging was the most likely candidate responsible for the presence of the potential barrier.

Figure 16 displays a spectrogram which illustrates some of these differential charging effects. The spacecraft "ground" is charged to a potential of about -100 V, as can be seen from the absence of ions at energies below about 100 eV. The bright band of electrons at low energies up to a few tens of eV is the photoelectron peak caused by spacecraft-emitted electrons returned to the detector by a potential barrier. The barrier height may be inferred from the transition energy between the photoelectrons and the ambient electrons. This transition energy can be inferred from the minimum in the count rate at about 100 eV as shown in the line plot of Figure 17. The distinct peaks above and below 100 eV indicate that the lower energy electrons come from one source (from the spacecraft), whereas the higher energy electrons come from a different source (the ambient plasma).

The very bright triangular streaks in the spectrogram in Figure 16 which occur at roughly this transition energy are electrons emitted and accelerated from differentially charged portions of the spacecraft. In Figure 17 these electrons appear as the very sharp spikes at ~ 100 eV. The triangular appearance of these streaks in the spectrogram is due to the rotation of the detector. The portion of the spacecraft which is charged differentially is emitting electrons over a range of kinetic energies. As the electrons leave this surface they are further accelerated by the local electric fields. Electrons with higher kinetic energies tend to travel in more-or-less straight lines, while electrons with lower initial kinetic energies will have their trajectories curved to a greater degree

by the electric fields. To detect the electrons with higher energies, the particle detector must be looking approximately in the direction of the differentially charged spot, while the lower energy electrons appear from a direction corresponding to the position of the barrier. Figure illustrates this configuration and shows the types of trajectories that can occur. This picture is in agreement with the electron streaks in the spectrogram which have been re-plotted against detector angle in Figure 19. The higher energy portion of the triangular streak occurs at a detector rotation angle when the detector is looking parallel to the spacecraft surface (The dark line in the ion data at this position in the spectrogram of Figure 16 is due to the presence of an obstruction on the solar array arm which blocks direct entrance of energetic ambient ions into the particle detector.) The low energy portion of the streak occurs when the detector is looking away from the spacecraft.

It is difficult in general to pin down exactly that portion of the spacecraft which is differentially charged. However, we have been able to identify the source of some of the electron spikes. One of the other experiments in the ATS-6 EME module is the University of Minnesota electron-proton spectrometer (Walker et al, 1975). One of the detector assemblies is a roughly 5 cm rotating cube finished with white paint. During several differential charging events, the sharp electron spikes as observed by the UCSD detector only appeared when both the UCSD detector and the Minnesota detector were each at unique rotation positions. The two detector rotation rates were not synchronous, so that the spikes appeared at what was essentially the beat frequency between the two rotation frequencies, or at the Minnesota frequency when the UCSD detector was fixed in position. We infer that the emitted photoelectrons or

ORIGINAL PAGE IS
OF POOR QUALITY

secondary electrons from the painted external surface of the Minnesota detector could only enter our detector when both detectors were oriented in a certain unique way, presumably because of a favorable electric field configuration at that time. (Johnson and Whipple, 1978)

4. WAYS OF IMPROVING LOW ENERGY PARTICLE MEASUREMENTS

In this section we make some suggestions as to how the measurements of low energy particle properties might be improved. We have four basic suggestions: (1) Improve the low energy resolution of particle detectors; (2) Design and build electrostatically clean spacecraft so as to reduce differential charging effects; (3) Control the spacecraft potential; (4) Make use of auxiliary measurements, particularly wave data.

(1) Better Low Energy Resolution.

The energy resolution of the ATS-6 instrument ($\Delta E/E$) was approximately 20%, which should be adequate for most studies. However, at low energies, below about 10 eV, both the energy level E and the width of the channel ΔE were affected by noise on the high voltage power supply. This noise resulted in modulation of the potential difference between the analyzer plates, so that in effect the energy levels and the width of the channels at low energies were also being modulated. In order to obtain quantitative results for the low energy particle measurements, it has been necessary to correct for this effect, which involves a demodulation of the data. This correction at best is somewhat uncertain, and this effect is probably the largest source of error in the low energy measurements on ATS-6.

A beneficial feature of the ATS-6 instrument which has helped in

getting at the low energy data is a transient response occurring in transitions from high to low energy steps. During such a transition, an offset is provided because of an unbalanced leakage current at the input to the analyzer supply. This offset decays away with a $1/(t+c)$ response. In the appropriate instrument mode, the slewing response slowly sweeps through energies that were not originally intended. The energy selection is therefore extended to around 1 eV. Comparison of the slewing effect in different instrument modes (i.e. different SCAN/DWELL modes) enables us to get a better estimate of the energy levels and widths at low energies. Unfortunately, the slewing effect is quite temperature dependent which makes its systematic use difficult.

On the SCATHA spacecraft, the UCSD instrument will have the high voltage power supply removed from three of the detectors. Consequently, we expect to get much better energy definition at low energies, down to about 0.1 eV.

An important aspect of low energy particle measurements is the laboratory calibration of the instrument. It is not safe to rely on the calculated performance parameters without checking them experimentally. For example, we have found that the electrostatic configuration of the post-analysis focusing lens and secondary electron suppressor has a marked effect on the electron detector characteristics. This effect is still not completely understood, but the behavior of the SCATHA instrument is well-documented in the laboratory calibrations, and we expect to be able to pin this problem down.

(2) Elimination of Differential Charging.

Some effects of differential charging of the ATS-6 spacecraft on particle data have been described in the previous section. The main effect

ORIGINAL PAGE IS
OF POOR QUALITY

ORIGINAL PAGE IS
OF POOR QUALITY

on low energy particle data is the exclusion of low energy plasma electrons by the potential barrier produced by differential charging, and the return of photoelectrons and secondary electrons to the spacecraft and to the particle detectors at low energies, also by the action of the barrier. The presence of the photoelectrons and secondary electrons can be confusing since it is easy to misinterpret their origin and assume that they are from the environmental plasma. We believe that this kind of erroneous interpretation has occurred on previous spacecraft (Grard, DeForest and Whipple, 1977).

Differential charging can be reduced or eliminated by either active experiments involving the deliberate emission of charged particles by the spacecraft in order to neutralize charged surfaces, or by a spacecraft design and construction program aimed at providing uniformly conducting surfaces. The latter approach has been taken on the GEOS and ISEE spacecraft, and appears to have been very successful in eliminating the phenomena of differential charging. The former approach of experimentally neutralizing charged dielectric surfaces has been observed during some ATS-6 active experiments involving the emission of ions by the experimental ion thruster and neutralizer on board (Olsen and Whipple, 1978). Figure 20 is a spectrogram during day 292 of 1976 when the ion thruster on ATS-6 was operated. Differential charging can be recognized by the bright band at low energies (up to about 100 eV) in the electron data. The top of this band is indicative of the magnitude of the differential potentials on the spacecraft. At 7:40 the ion thruster neutralizer is ignited, and the differential potentials are reduced but not eliminated. This is shown by the drop in energy of the top of the photoelectron band. At 8:05 the main thruster ignites, and the bright band disappears, indicating that the

differential charging has been eliminated. Our interpretation is that the neutralizer only emits enough ions to reduce the differential charging, not eliminate it, whereas the main thruster provides a large source of low energy charge exchange cesium ions which are drawn to the negatively charged surfaces in sufficient quantity to eliminate the differential charging.

(3) Control of Spacecraft Potential.

The active experiments on the ATS-5 and ATS-6 spacecraft have also been used to modify the spacecraft potential. The presence of even a moderate spacecraft potential of a few tens of volts has a serious effect on low energy particle data, since the spacecraft will repel all the particles with the same electric charge as the spacecraft so that any with energies below the spacecraft potential cannot be observed. The data describing the attracted species is also degraded since the particles are accelerated to higher energies where the energy bandwidth is broader.

During the fall of 1974 the ATS-6 ion engine was operated for a period of 92 hours. The engine was ignited in the latter stages of a magnetospheric substorm when the spacecraft was charged to about -50 volts. (The spectrogram of Figure 20 is during the initial period of this operation.) The ignition of the neutralizer at 7:40 brought the spacecraft potential to within a few volts of the ambient plasma potential. After the main thruster was fired, the potential of the spacecraft stabilized at about -4 or -5 volts. This potential was maintained throughout the 92-hour operation in spite of the fact that several magnetospheric substorms (recognized by particle injections) occurred during this time. During similar storms outside this time period, the spacecraft charged to several hundred volts negative and experienced severe differential charging effects. The

ORIGINAL PAGE IS
OF POOR QUALITY

improvement in the low energy ion data during this operation can be seen from the appearance of ions counts at low energies after 7:40 in Figure 20. Before that time the low energy ions were accelerated to about 50 eV by the attractive spacecraft potential.

A number of other experiments with the thrusters and neutralizers on the ATS-5 and ATS-6 spacecraft have demonstrated the possibility and usefulness of modifying the spacecraft potentials by particle emission. Current balance calculations show that an emission current on the order of a few microamperes is sufficient in most cases to discharge the spacecraft. It is not necessary to completely discharge the spacecraft to zero volts in order to get reasonably good low energy particle data. A few volts positive or negative seems to be sufficient; better yet would be a slow (few minute) modulation or sweep of the spacecraft potential between a few volts positive and negative. This would enable data to be obtained for both ions and electrons under conditions of both an attractive and repulsive spacecraft, and would permit a useful comparison and mutual calibration.

(4) Use of Auxiliary Data.

Our final suggestion is to make use of as much auxiliary information as possible from other experiments. Detection of plasma waves is a particularly valuable source of information since this can provide an independent check of particle parameters such as density, temperature, and in some cases, ion species. The characteristics of plasma waves are in general determined by the plasma properties over a fairly large volume compared to the dimensions of the spacecraft. Consequently, such measurements are usually unaffected by the presence of the spacecraft and associated plasma perturbations in its vicinity.

In his thesis, Mauk (1978) has used wave data obtained simultaneously from the UCSD particle detectors and the UCLA magnetometer on ATS-6 to infer the low energy ion density. The waves were propagating, electromagnetic Alfvén/ion cyclotron waves with frequencies in the range of a few Hz. These waves were detected by the particle instruments as a modulation in the count rates of the ions at particular energies, and by the magnetometer as a modulation in the magnetic field in both magnitude and direction. The dispersion relation for the waves combined with Maxwell's curl E equation provide a relation between the measured energy and magnetic field modulations which depends on the ion density. Thus it was possible to infer the density with about a factor of two uncertainty. In this particular instance the mass dependence drops out of the calculation, so that the density determination is to first order independent of the kind of ion. However, Mauk was able to place upper limits on the amount of heavy ions from the properties of the ion wave propagation.

Other kinds of plasma waves, and in particular observations of plasma resonances, can provide information on the plasma density and temperature. Observations of plasma resonances from the ISIS satellites have been especially fruitful in yielding electron densities and scale heights at the satellite location, as well as remote densities through the sounder capabilities (Crawford et al, 1967). McAfee (1968) has shown how the structure of the plasma resonance observed as a result of stimulation on the spacecraft can provide both the local electron density and temperature. This kind of observation is being obtained on both the GEOS and ISEE spacecraft and is turning out to be an extremely valuable complement to the more conventional particle data (e.g. Gurnett et al, 1978; Christiansen et al, 1978).

REFERENCES

- Christiansen, P., P. Gough, E. Martelli, J. J. Bloch, N. Cornilleau, J. Etcheto, R. Gendrin, C. Beghin, P. Decreau, D. Jones, GEOS Observations of Electrostatic Waves and their Relations with Plasma Parameters, 13th ESLAB Symposium, Innsbruck, June, 1978.
- Crawford, F. W., R. S. Harp, T. D. Mantei, On the Interpretation of Ionospheric Resonances Stimulated by Alouetta 1, J. Geophys. Res. 72, 57, 1967.
- DeForest, S. E., Spacecraft Charging at Synchronous Orbit, J. Geophys. Res. 77 651, 1972.
- Frank, L. A., Personal Communication.
- Grard, R. J. L., S. E. DeForest, E. C. Whipple, Comment on Low Energy Electron Measurements in the Jovian Magnetosphere, Geophys. Res. Letters 4, 247, 1977.
- Gurnett, D. A., R. R. Anderson, F. L. Scarf, R. W. Fredricks, E. J. Smith, A Survey of Plasma Wave Observations from ISEE 1 and 2, 13th ESLAB Symposium, Innsbruck, June, 1978.
- Johnson, B., E. C. Whipple, Characteristics of Differential Charging on ATS-6, Spacecraft Charging Technology Conference, Colorado Springs, October, 1978.
- Mandell, M. J., I. Katz, G. W. Schnuelle, P. G. Steen, J. C. Roche, The Decrease in Effective Photocurrents due to Saddle Points in Electrostatic Potentials Near Differentially Charged Spacecraft, IEEE Annual Conference on Nuclear and Space Radiation Effects, Albuquerque, July, 1978.
- Mauk, B. H., Alfvén/Ion Cyclotron Waves and the Ion Cyclotron Instability in the Earth's Magnetosphere, Ph.D. Thesis, University of California at San Diego, April, 1978.
- Mauk, B. H., C. E. McIlwain, UCSD Auroral Particles Experiment, IEEE Transactions on Aerospace and Electronic Systems, AES-11, 1125, 1975.
- McAfee, J. R., Ray Trajectories in an Anisotropic Plasma near Plasma Resonance, J. Geophys. Res., 73, 5577, 1968.
- McPherson, D. A., D. P. Cauffman, W. Schober, Spacecraft Charging at High Altitudes - The SCATHA Satellite Program, Spacecraft Charging by Magnetospheric Plasma, Progress in Astronautics and Aeronautics, 47, A. Rosen, ed., 1976.
- Olsen, R. C., E. C. Whipple, Operations of the ATS-6 Ion Engine, Spacecraft Charging Technology Conference, Colorado Springs, October, 1978.
- Scarf, F. L., Personal Communication.
- Walker, R. J., K. N. Erickson, R. L. Swanson, J. R. Winckler, Synchronous Orbit Trapped Radiation Studies with an Electron-Proton Spectrometer, IEEE Transactions on Aerospace and Electronic Systems, AES-11, 1131, 1975.

- Whipple, E. C., Observation of Photoelectrons and Secondary Electrons Reflected from a Potential Barrier in the Vicinity of ATS 6, J. Geophys. Res., 81, 715, 1976.
- Whipple, E. C., J. W. Hirman, R. Ross, A Satellite Ion-Electron Collector; Experimental Effects of Grid Transparency, Photemission, and Secondary Emission, ESSA Tech. Rept., ERL No. 99-AL1, 1968.
- Whipple, E. C., L. W. Parker, Effects of Secondary Electron Emission on Electron Trap Measurements in the Magnetosphere and Solar Wind, J. Geophys. Res., 74, 5763, 1969.
- Whipple, E. C., J. M. Warnock, R. H. Winkler, Effect of Satellite Potential on Direct Ion Density Measurements Through the Plasmopause, J. Geophys. Res. 79, 179, 1974.

TABLES AND FIGURES

Table 1 - Some Measurements of Satellite PotentialFigures

1. Electron density versus temperature for various Debye lengths.
2. Secondary electron yields for electron impact.
3. Secondary electron yields for proton impact.
4. Magnetic field versus temperature for various gyro-radii.
5. Experimental ion currents as OGO 1 traverses the plasmopause.
6. Ion current from OGO 1 in the earth's shadow.
7. Ion current from OGO 1 in sunlight illustrating photoemission.
8. Ion current from OGO 1 illustrating secondary emission effects.
9. Electron current from OGO 1 illustrating secondary emission effects.
10. Change in OGO 1 ion current cut-off potential through plasmopause.
11. Phase space density of electrons and protons before and during eclipse.
12. Experimental electron current from IMP 2 in the solar wind.
13. The ATS-6 spacecraft.
14. Spectrogram showing ATS-6 eclipse data on October 2, 1975.
15. Potential contours around a partially illuminated "octagonal sphere" showing saddle point at approximately -25 volts.
16. Spectrogram of ATS-6 data on September 5, 1974, showing differential charging effects. The change in intensity of the the electron data at Step 16 (100 eV) is due to a calibration effect.
17. A line plot of ion and electron count rates versus time and energy (dotted line) on September 5, 1974, showing spikes of electrons coming from differentially charged areas on the spacecraft.
18. Schematic illustration of how electrons from differentially charged areas follow different trajectories to the UCSD detector.
19. Plot of the distribution functions of electrons from differentially charged areas versus detector rotation angle illustrating the energy/angle correlation.
20. Spectrogram showing the effects of ion thruster and neutralizer operations on ATS-6 potential and differential charging.

TABLE 1.

SOME MEASUREMENTS OF SATELLITE POTENTIAL

Satellite	Launch Date	Experiment	Satellite Potential & Comments
Sputnik 3	5/15/58	Ion Traps	Negative to -6 volts
Explorer 8	11/3/60	Ion & Electron Traps	Normal ^a No solar cells, some effect from r.f. probe
Discoverer 32	10/13/61	Ion Trap	Normal ^a
Cosmos 2	4/6/62	Langmuir Probe & Ion Traps	Negative potential increased by positive potentials on outer grids of traps.
Air Force Satellite	4/17/62	Ion Trap	Negative to -20 volts
Ariel 1	4/26/62	Langmuir Probes	Normal ^a up to -1.0 volt
Explorer 17	4/3/63	Langmuir Probe	Normal ^a up to -1.0 volt at night
Tiros 7	6/19/63	Langmuir Probe	Normal ^a . Negative solar cells.
IMP A(Expl. 18)	11/27/63	Electron Trap	1-2 volts positive, Positive solar cells
Explorer 20	8/25/64	Langmuir Probe	Negative to -8 volts, Positive solar cells
OGO 1	9/5/64	I&E Traps Mass Spectr.	Negative to -15 volts, Positive solar cells
IMP B(Expl. 21)	10/4/64	Electron Trap	1-2 volts positive, Positive solar cells
Explorer 22	10/10/64	Langmuir Probe	Negative, exceeding -4 volts at times. Some positive solar cells
Explorer 27	4/29/65	Langmuir Probe	Negative to -8 volts. Some solar cell terminals coated
IMP C(Expl. 28)	5/29/65	Electron Trap	1-2 volts positive, Positive solar cells.
OGO 2	10/14/65	Ion, Electron Trap Mass Spectr.	Negative to -3 volts, solar cell terminals coated.

^a"Normal" means a few tenths of a volt negative near the earth.

ORIGINAL PAGE IS
OF POOR QUALITY

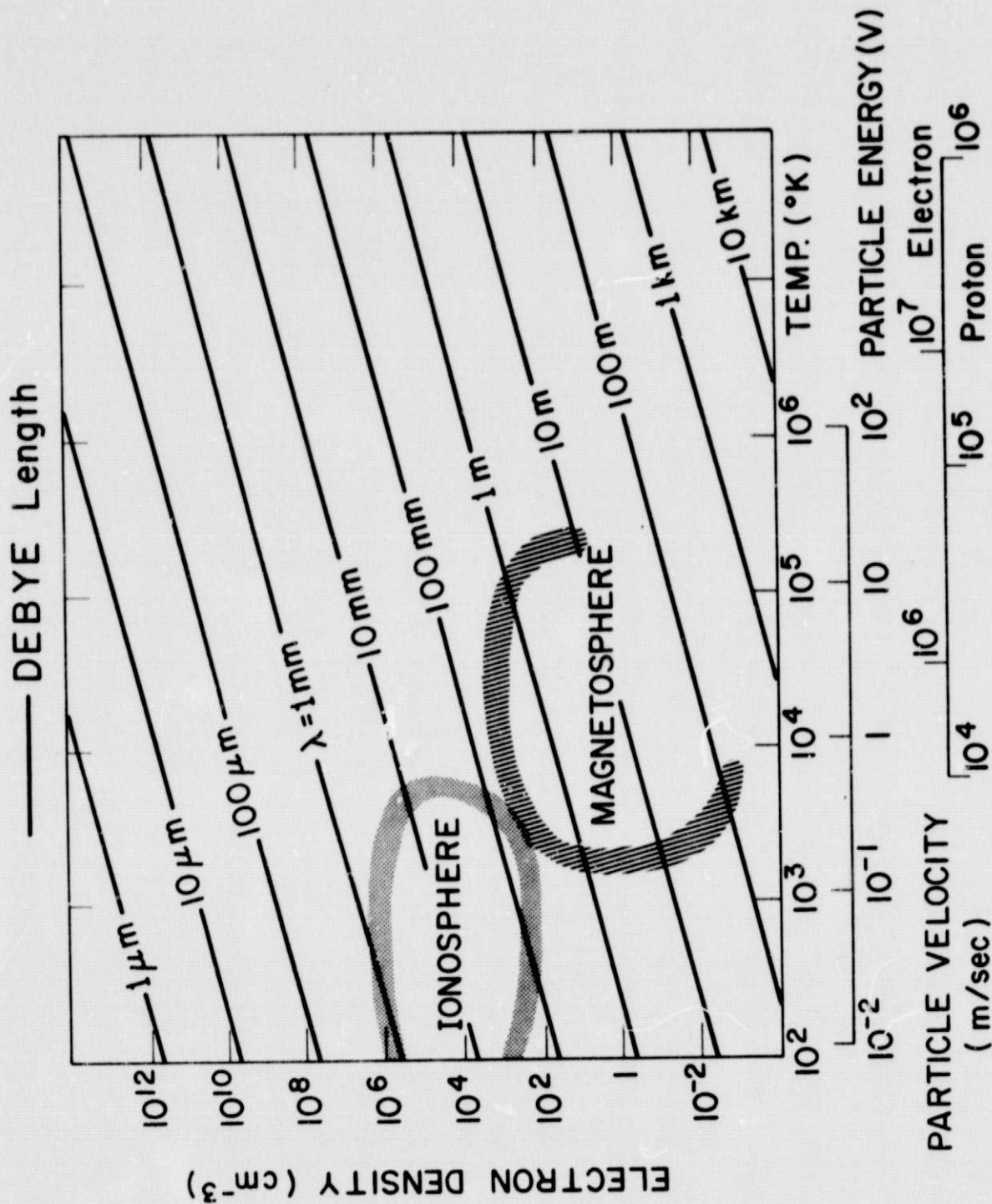


FIGURE 1



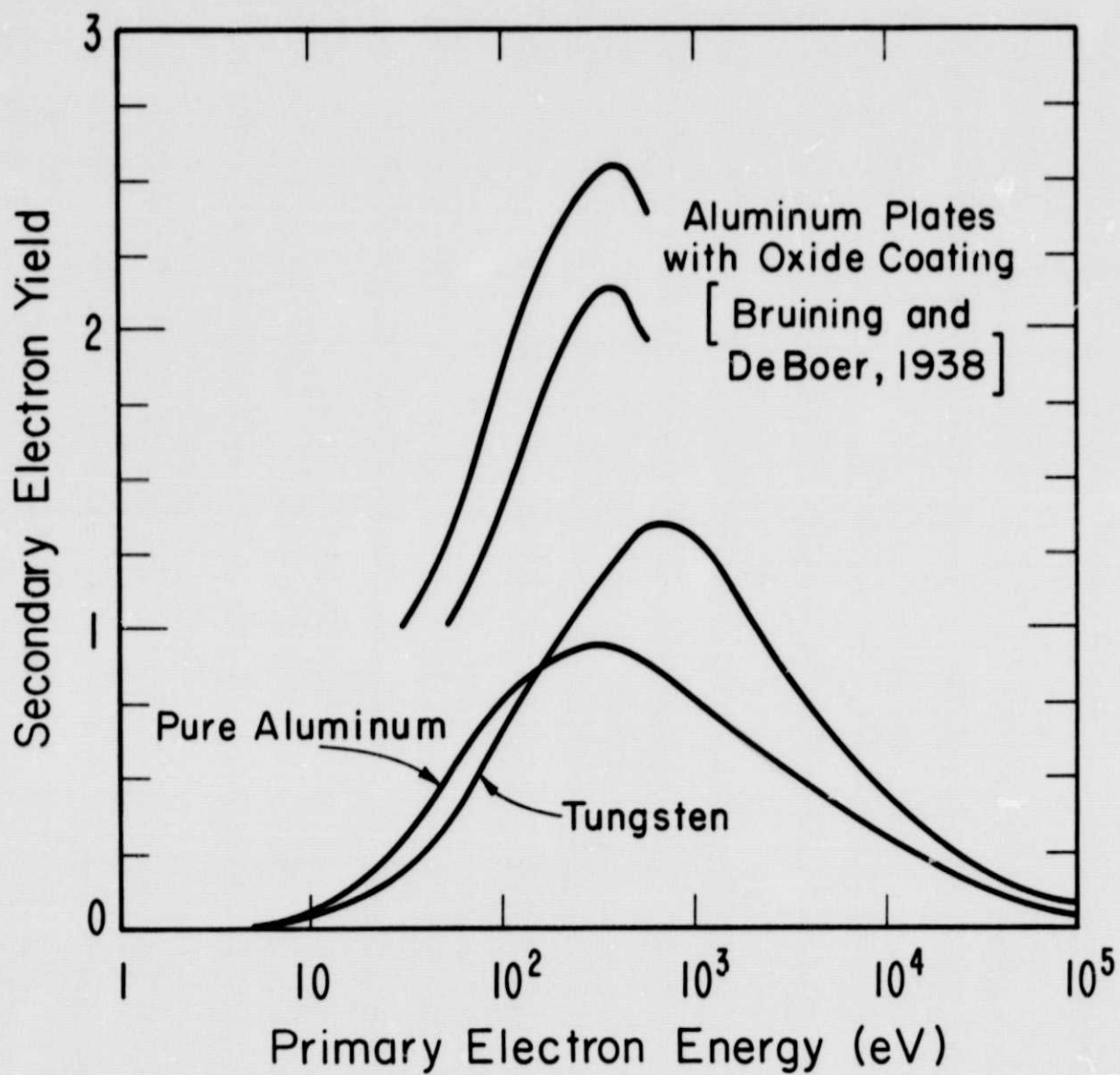


FIGURE 2

SECONDARY YIELD OF ELECTRONS FOR PROTON IMPACT AT ENERGIES ABOVE 1 KEV

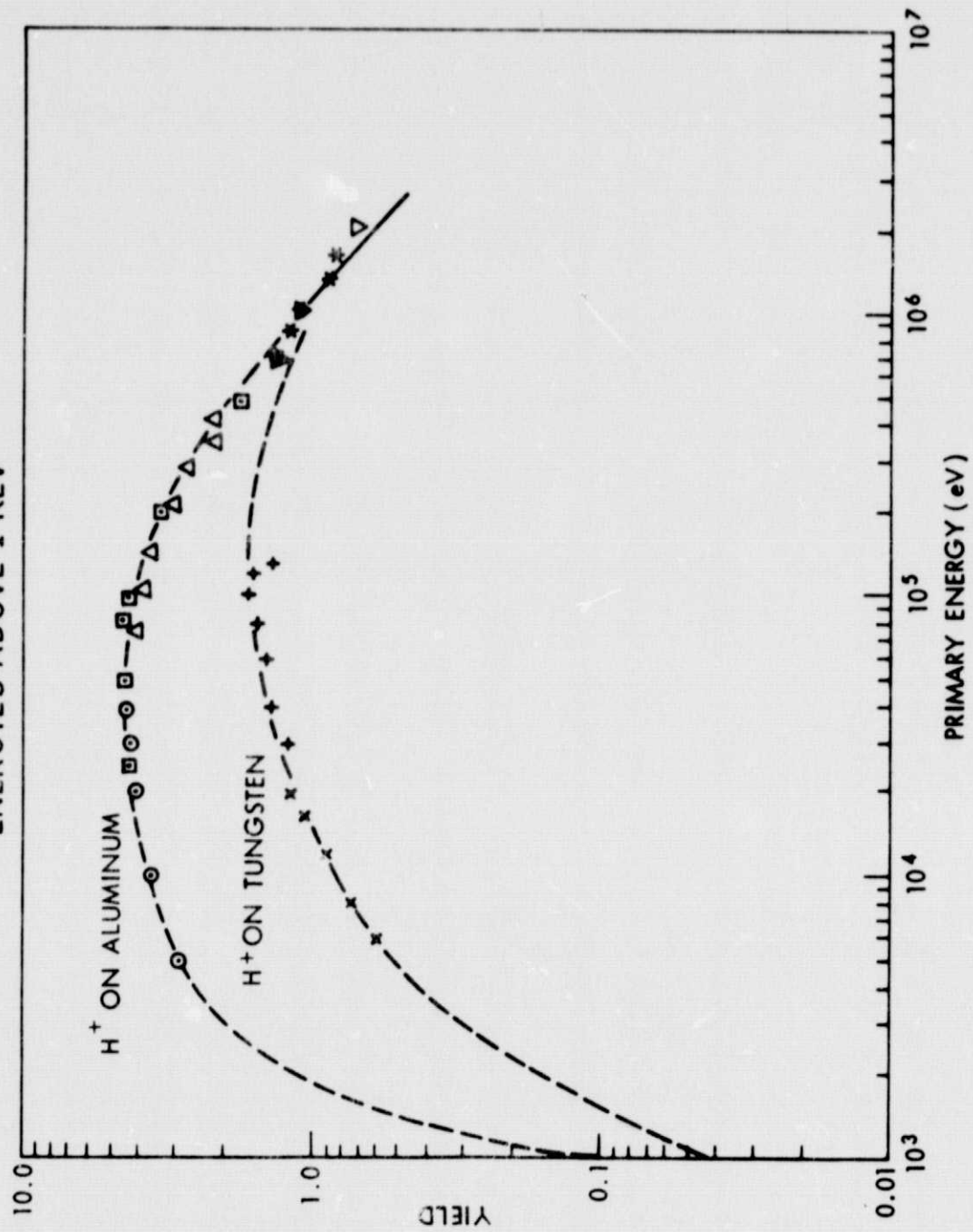


Figure 3

ORIGINAL PAGE IS
OF POOR QUALITY

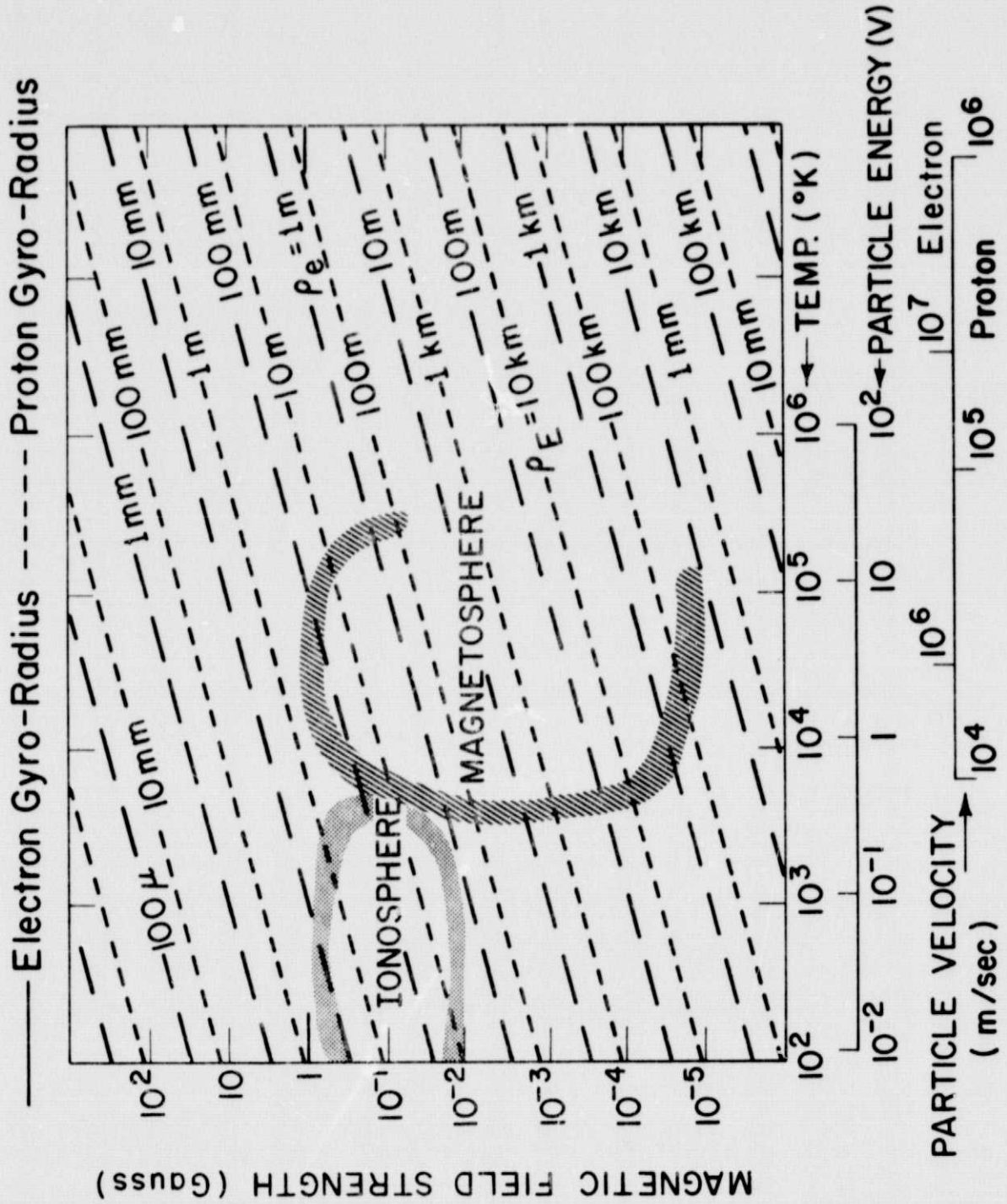


FIGURE 4



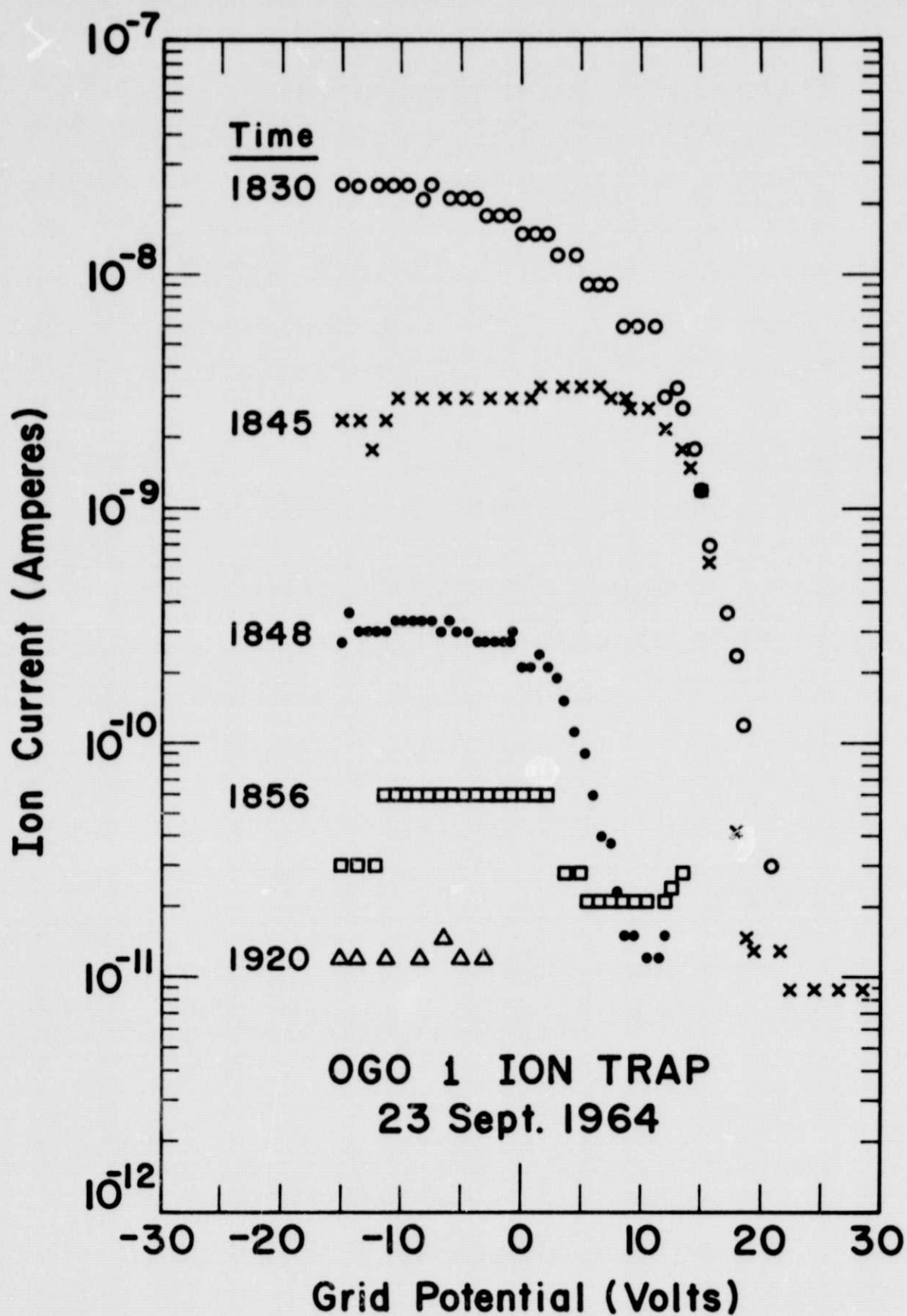


FIGURE 5

Ion Mode in Eclipse, 1910 UT 26 Mar 1965

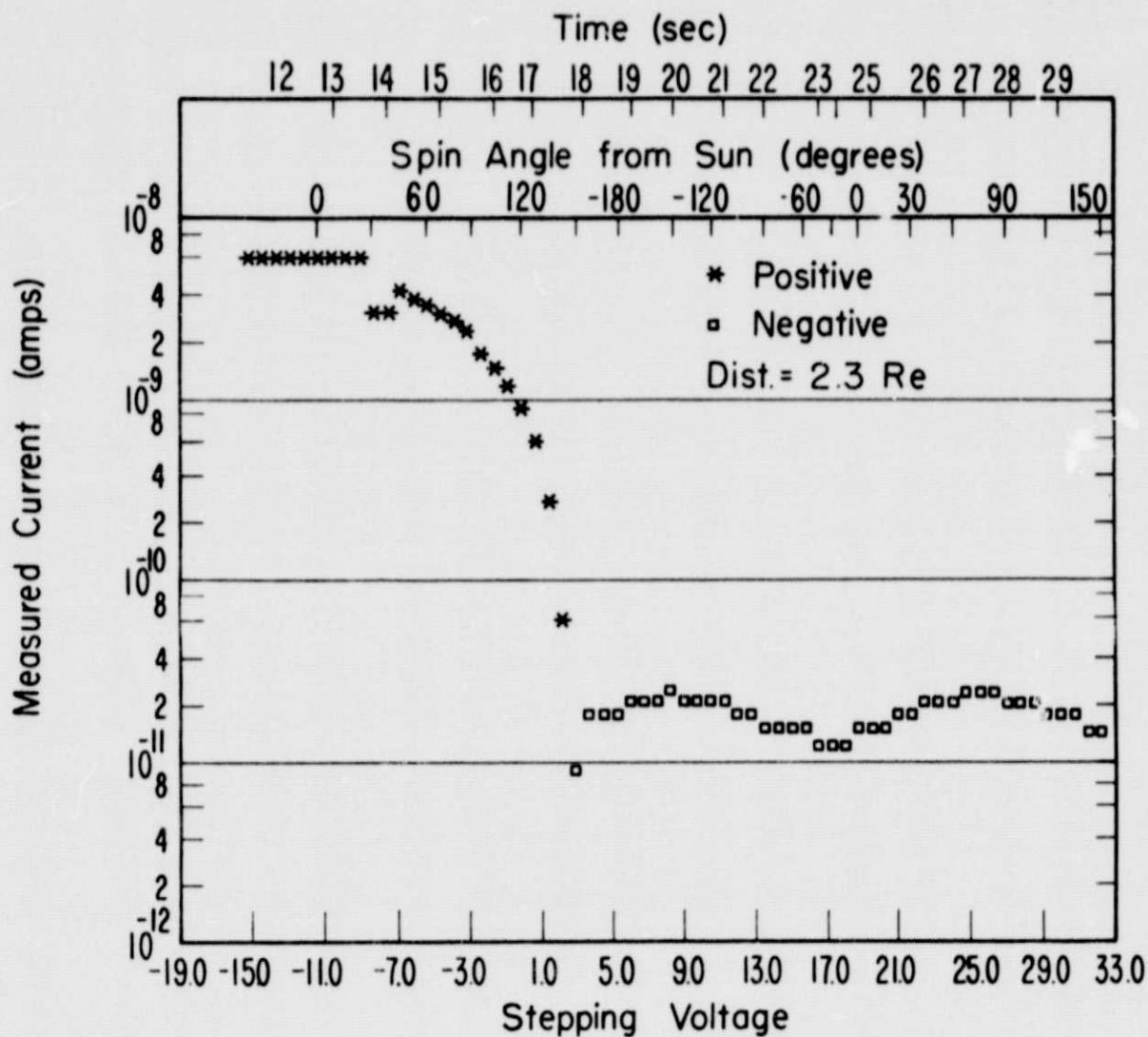


FIGURE 6

Ion Mode in Sunlight, 1915 UT 26 Mar. 1965

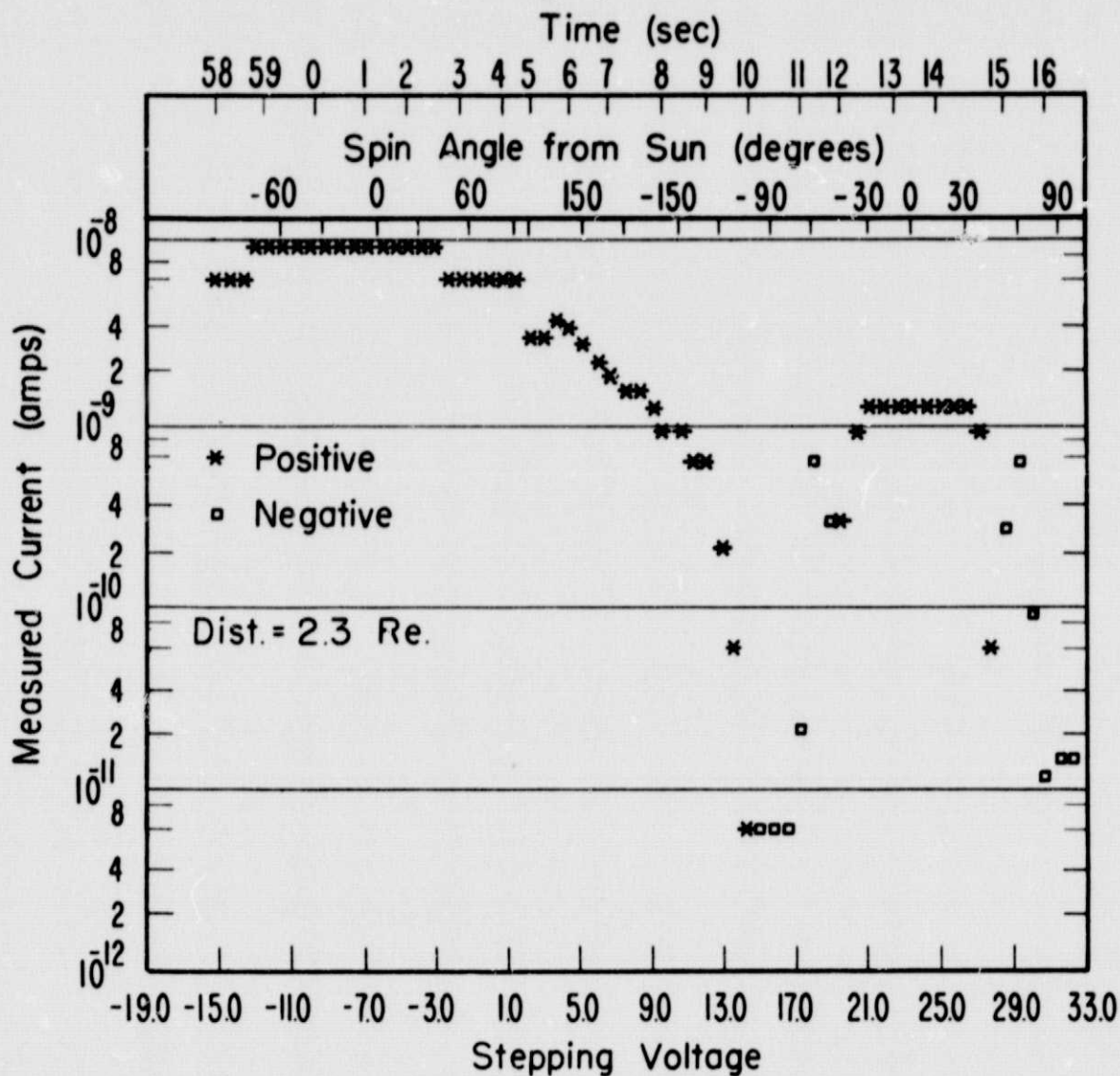


FIGURE 7

Ion Mode, 1207 UT 7 Dec 1964

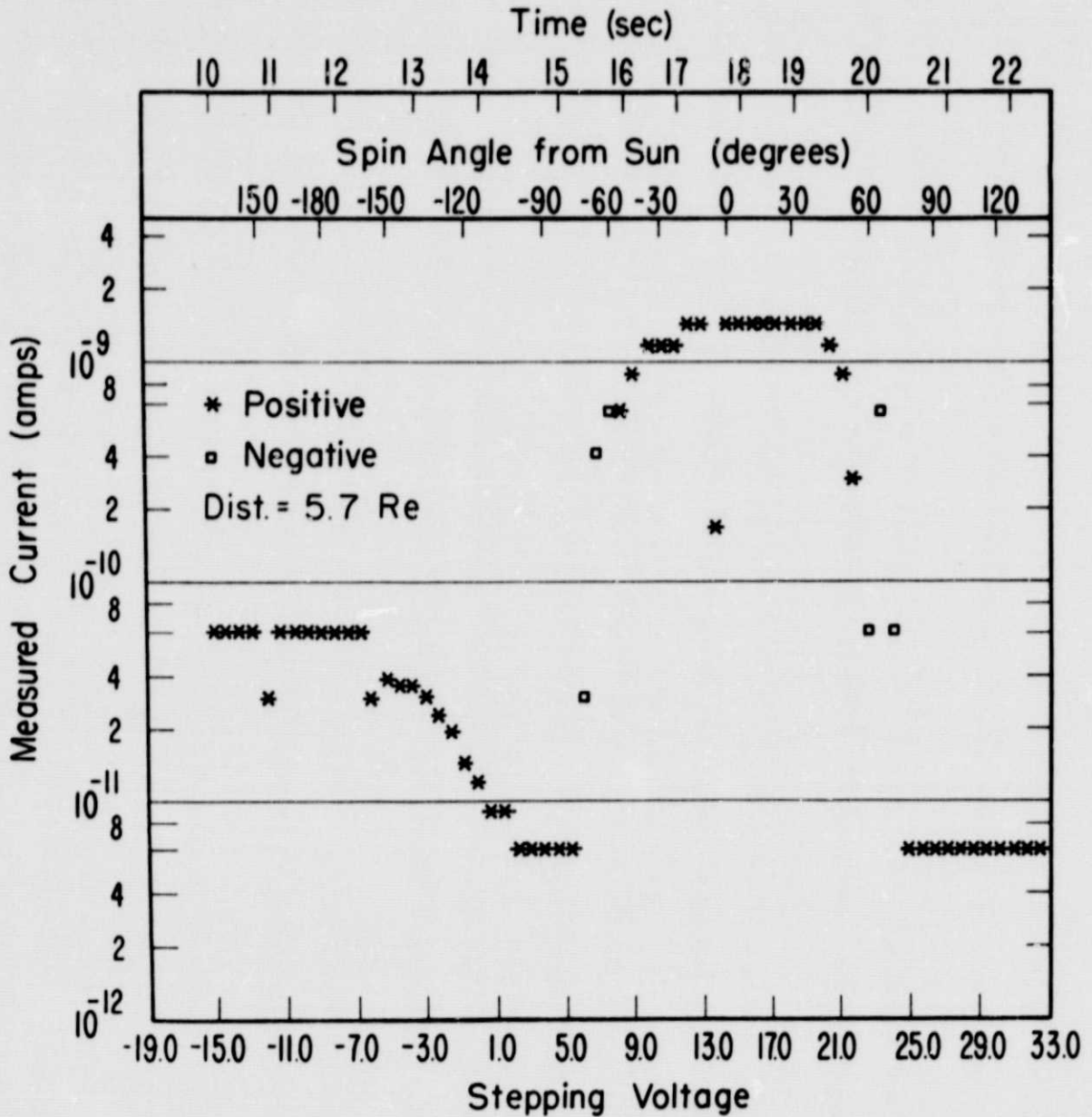


FIGURE 8

Electron Mode, 1208 UT 7 Dec 1964

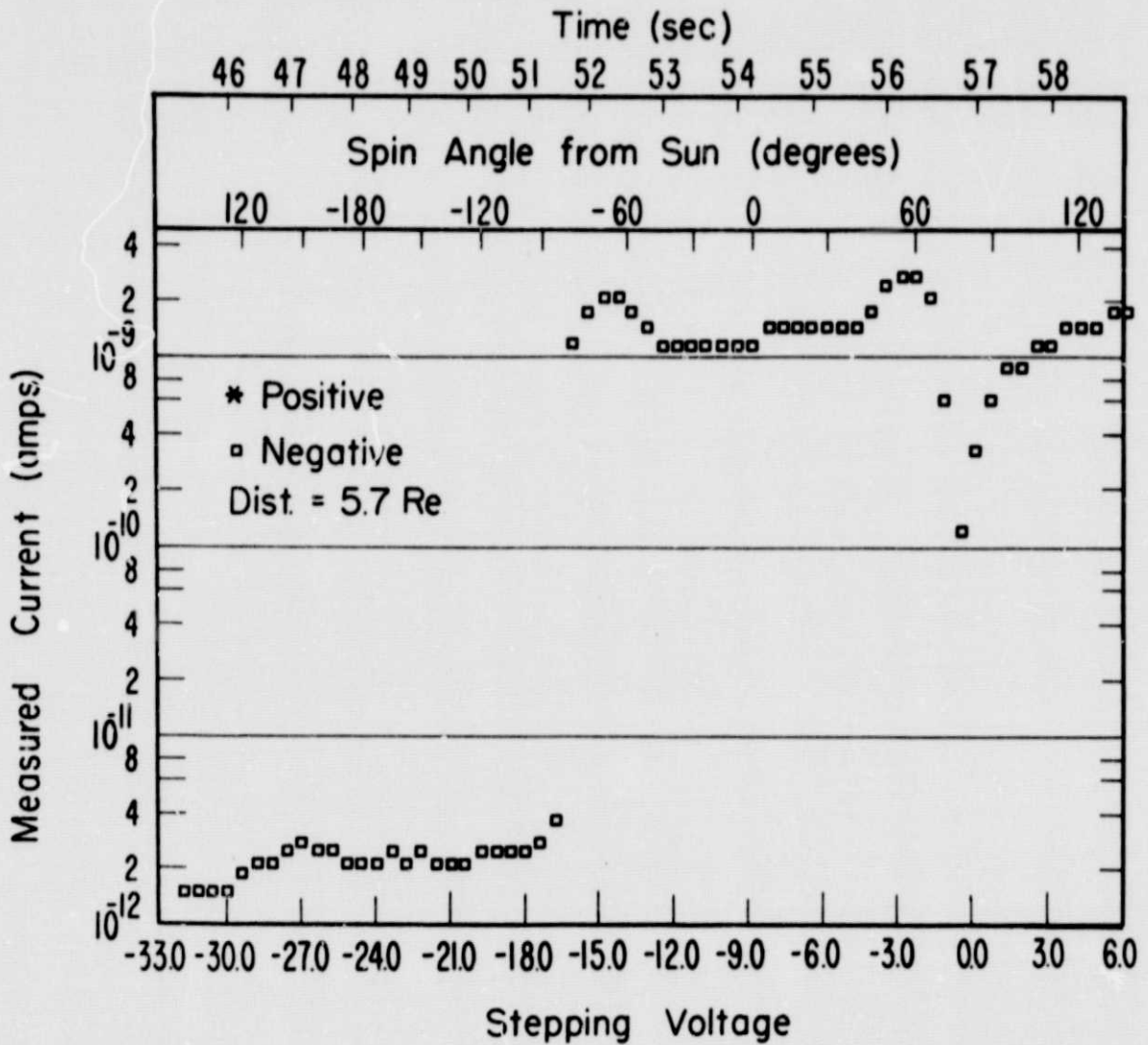


FIGURE 9

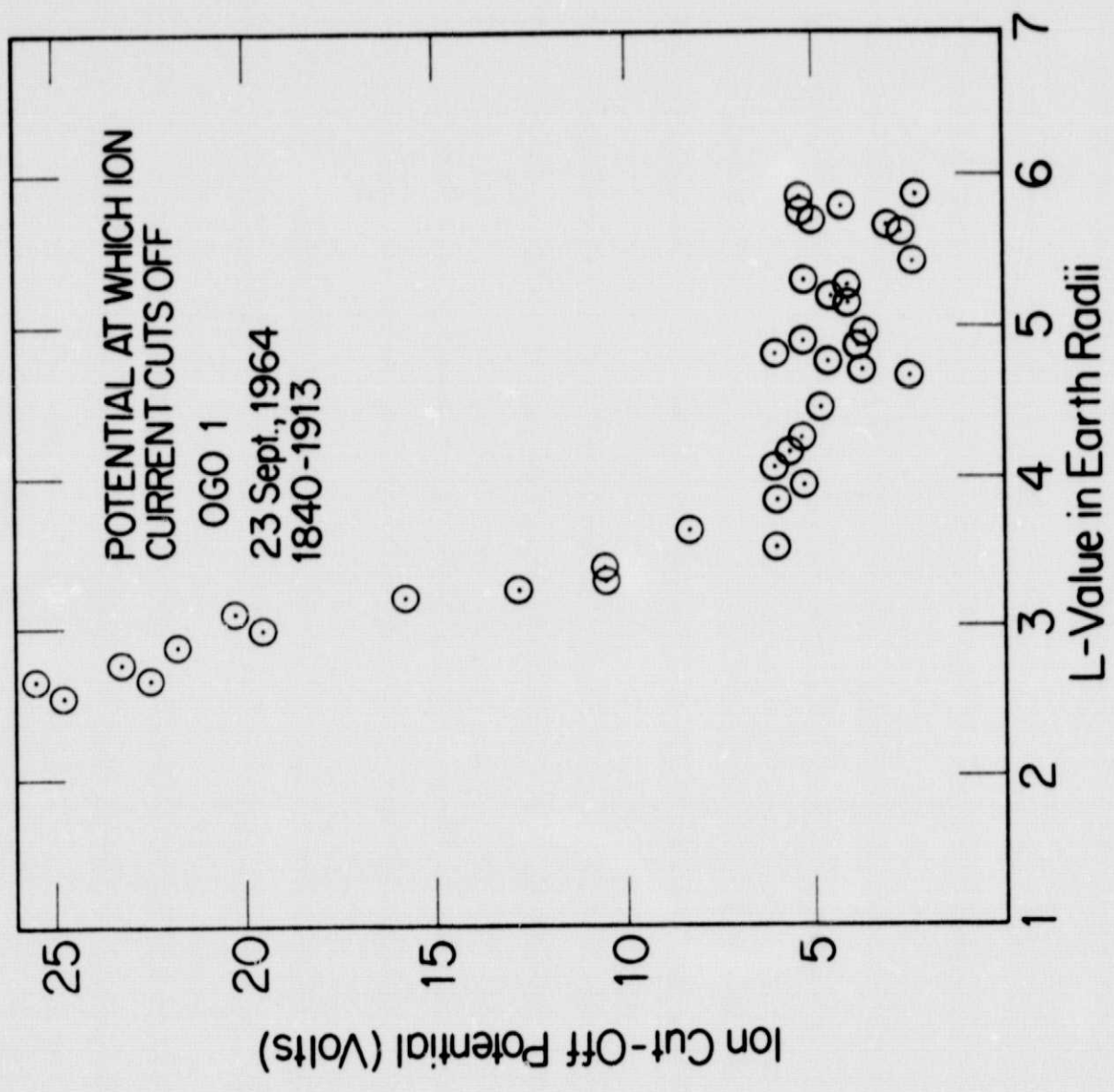


FIGURE 10

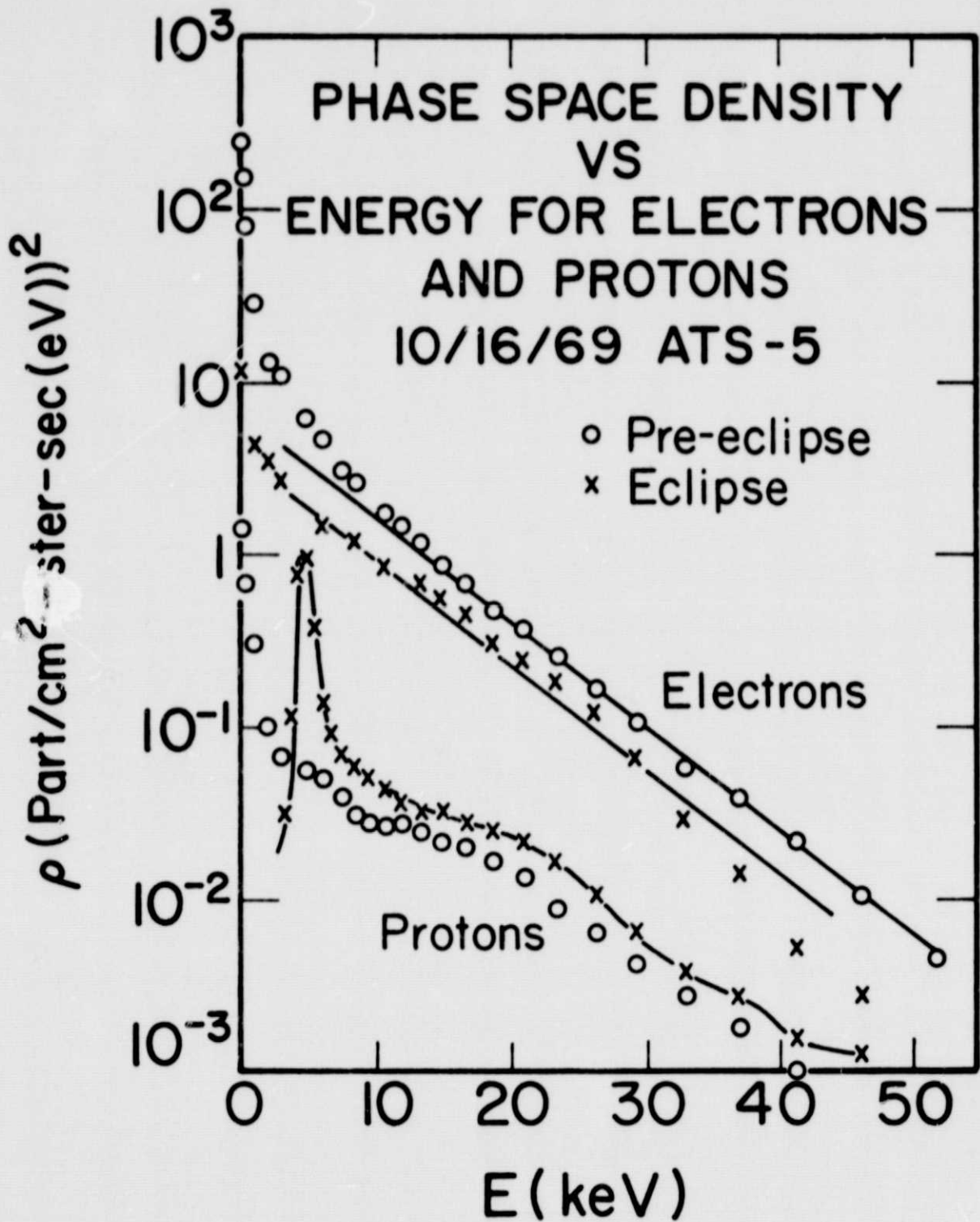


FIGURE 11

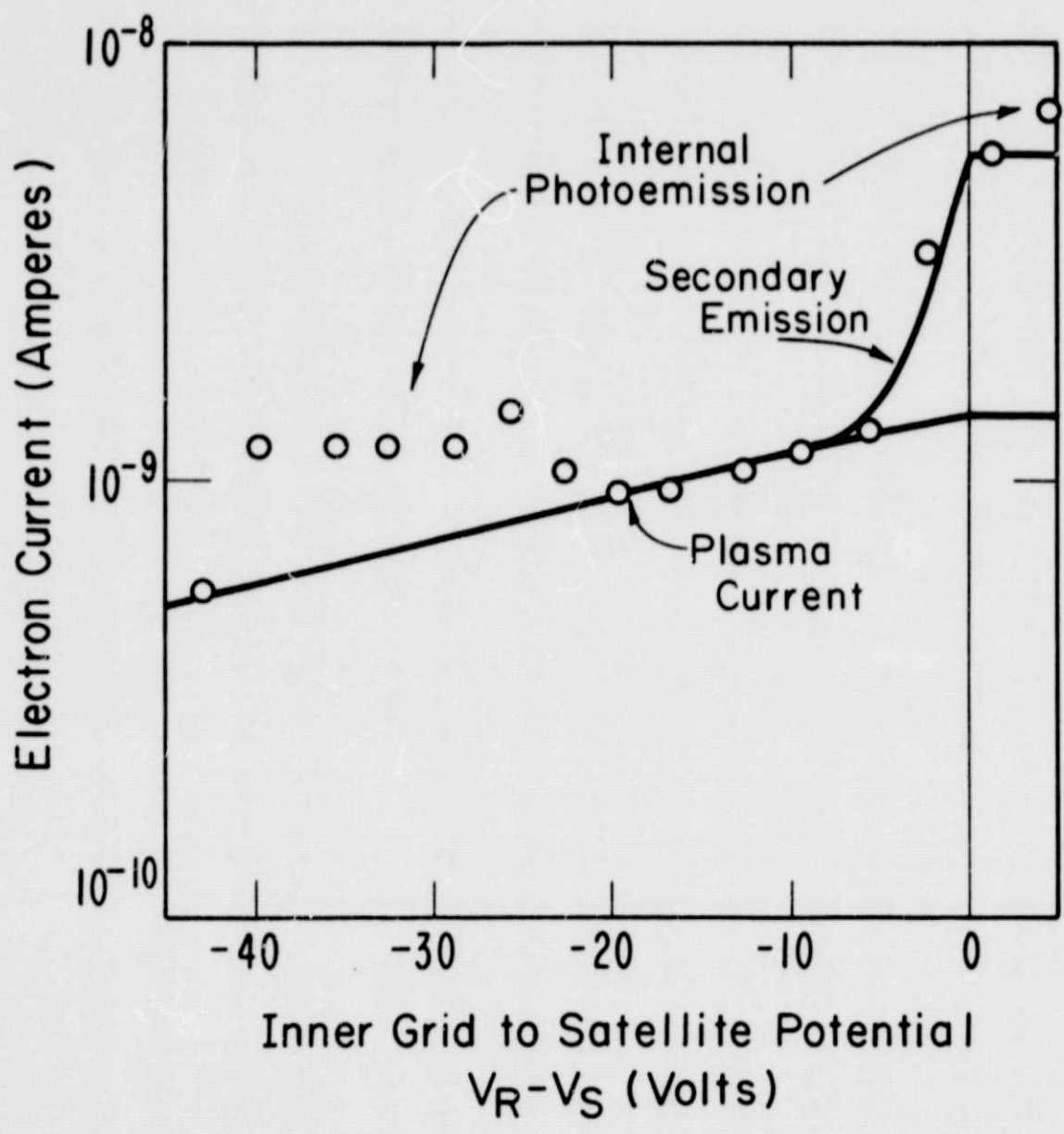


FIGURE 12

ORIGINAL PAGE IS
OF POOR QUALITY

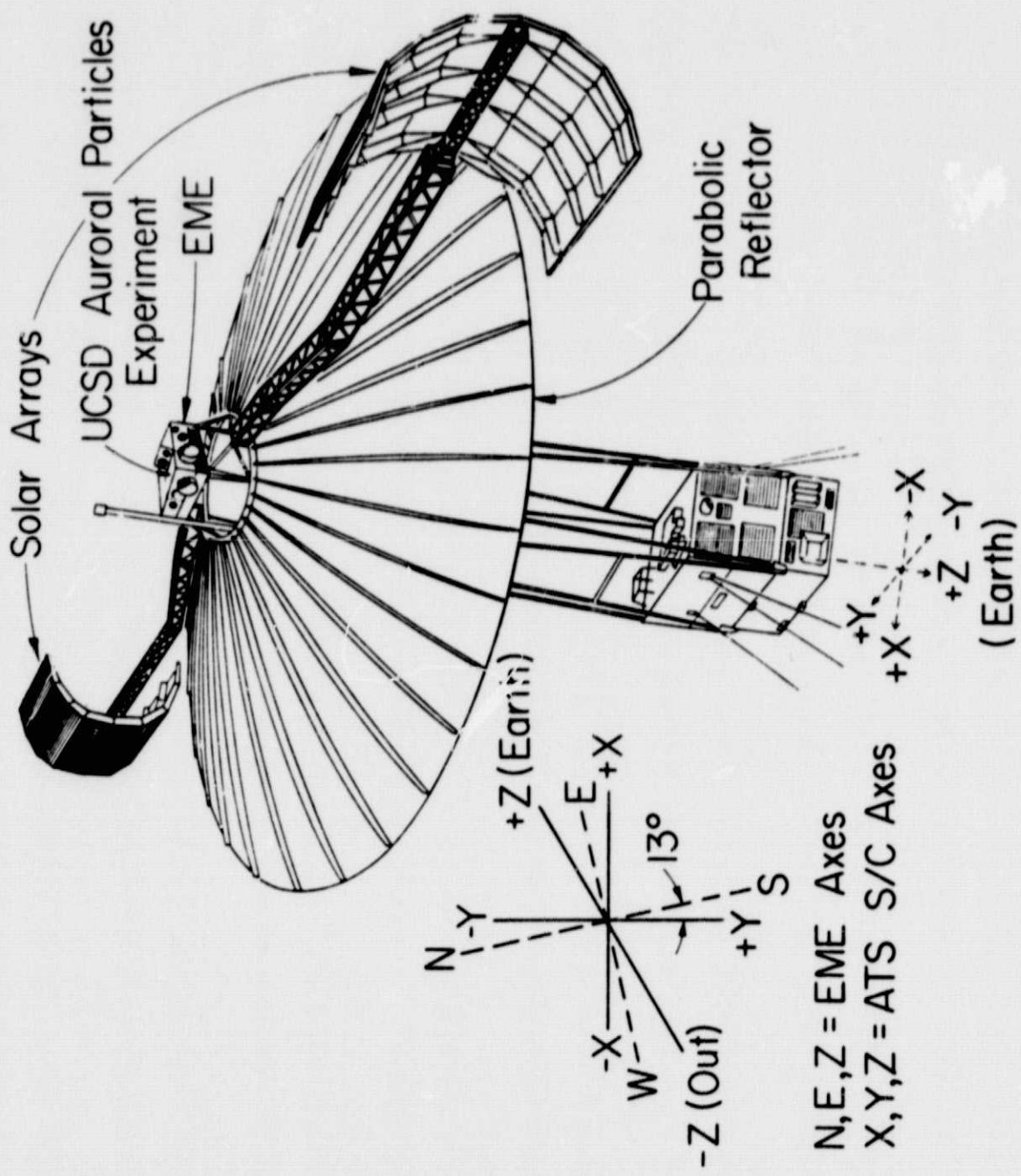
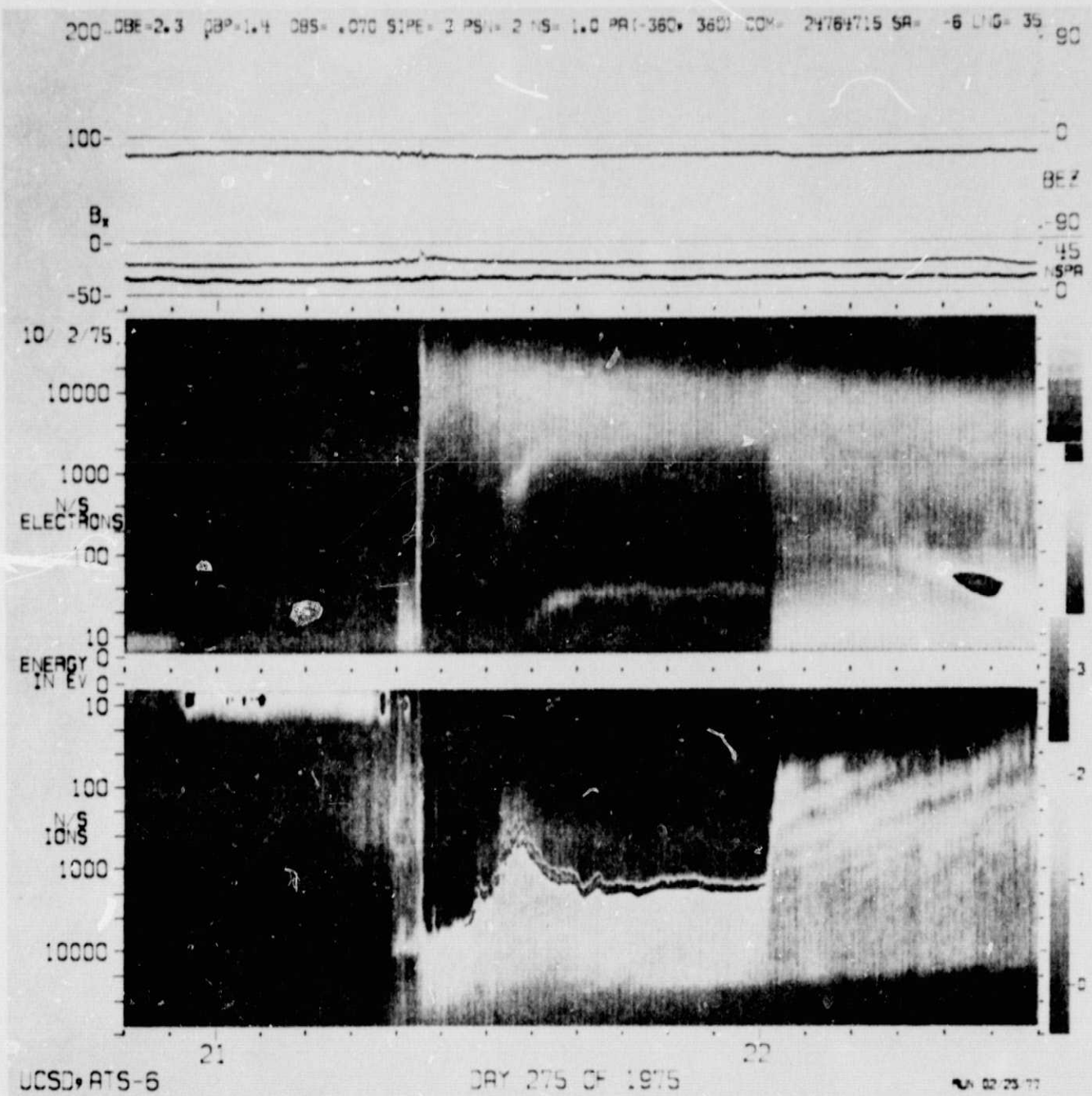


FIGURE 13



Spectrogram 1. ATS-6: Eclipse with Injection of Hot Plasma; 10/2/75

FIGURE 14

ORIGINAL PAGE IS
OF POOR QUALITY

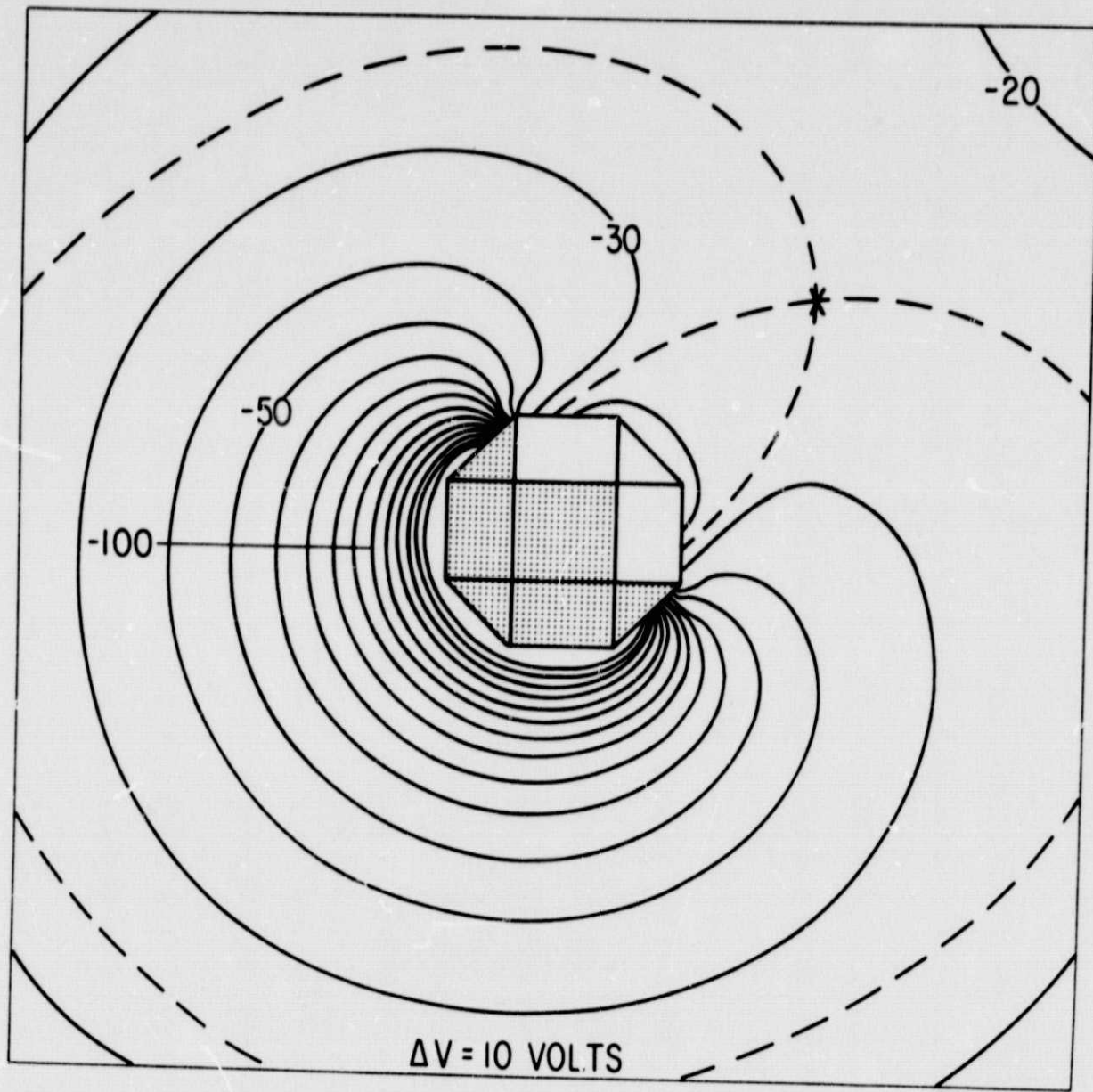


FIGURE 15

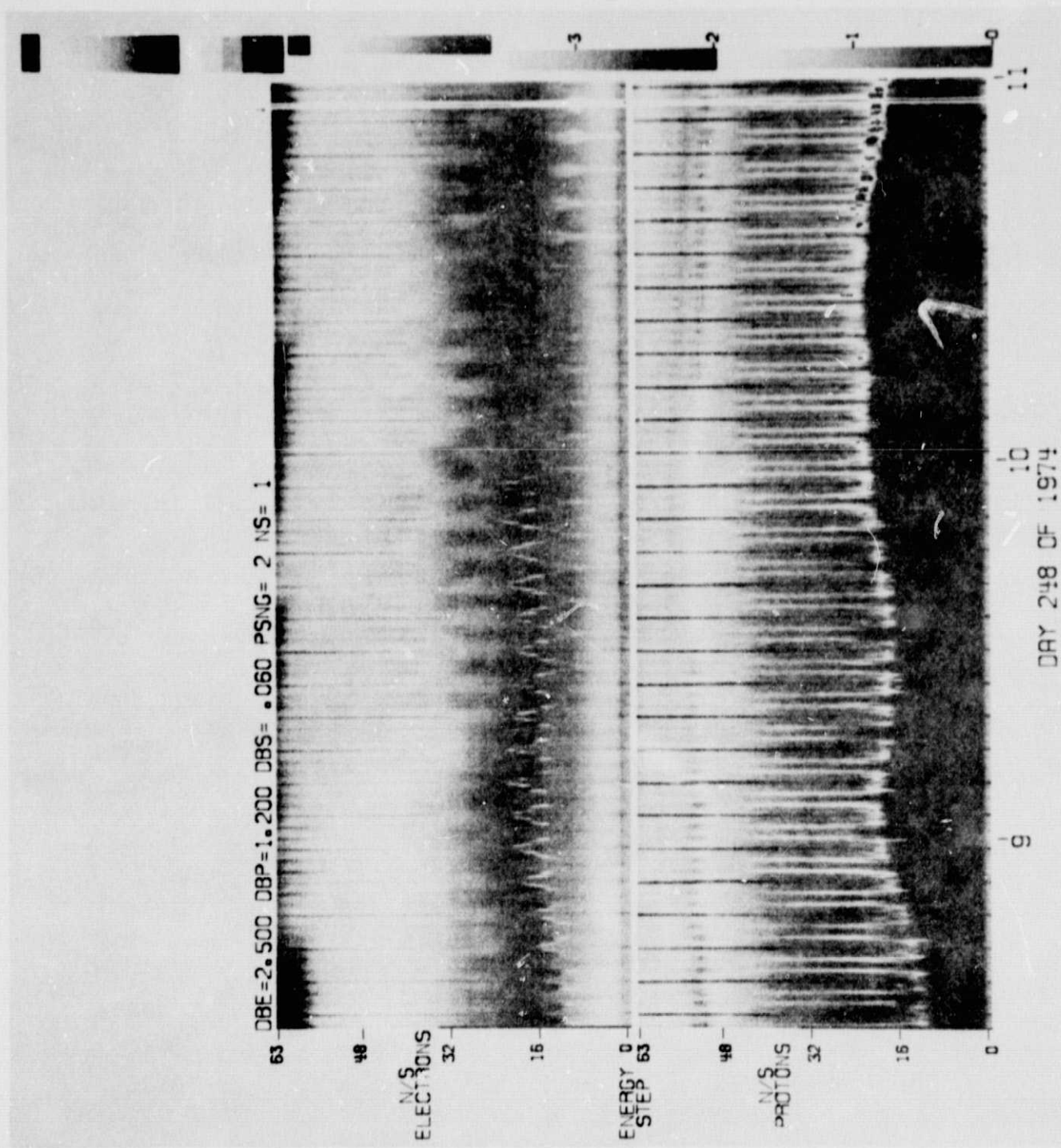


FIGURE 16

ORIGINAL PAGE IS
OF POOR QUALITY

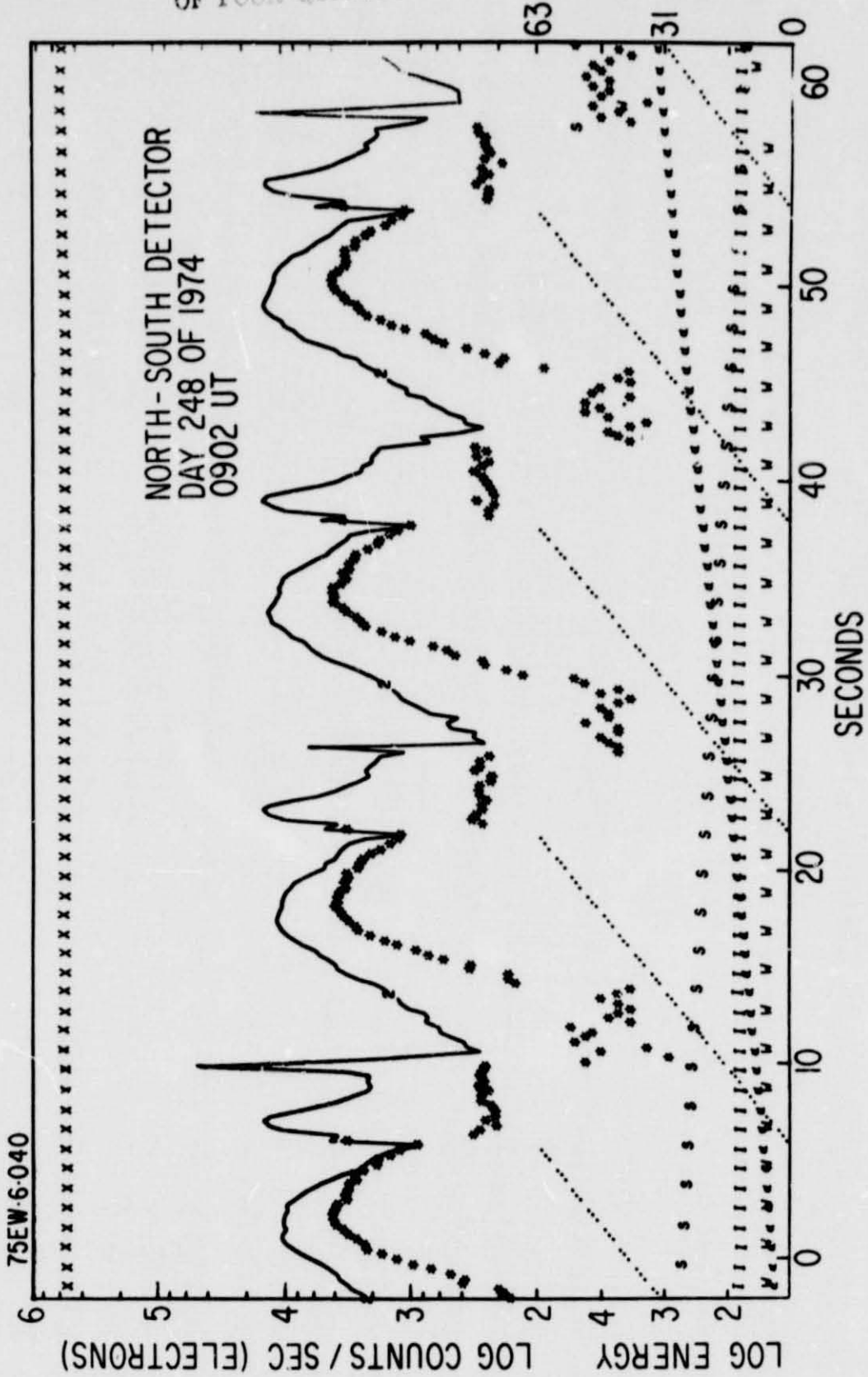


FIGURE 17

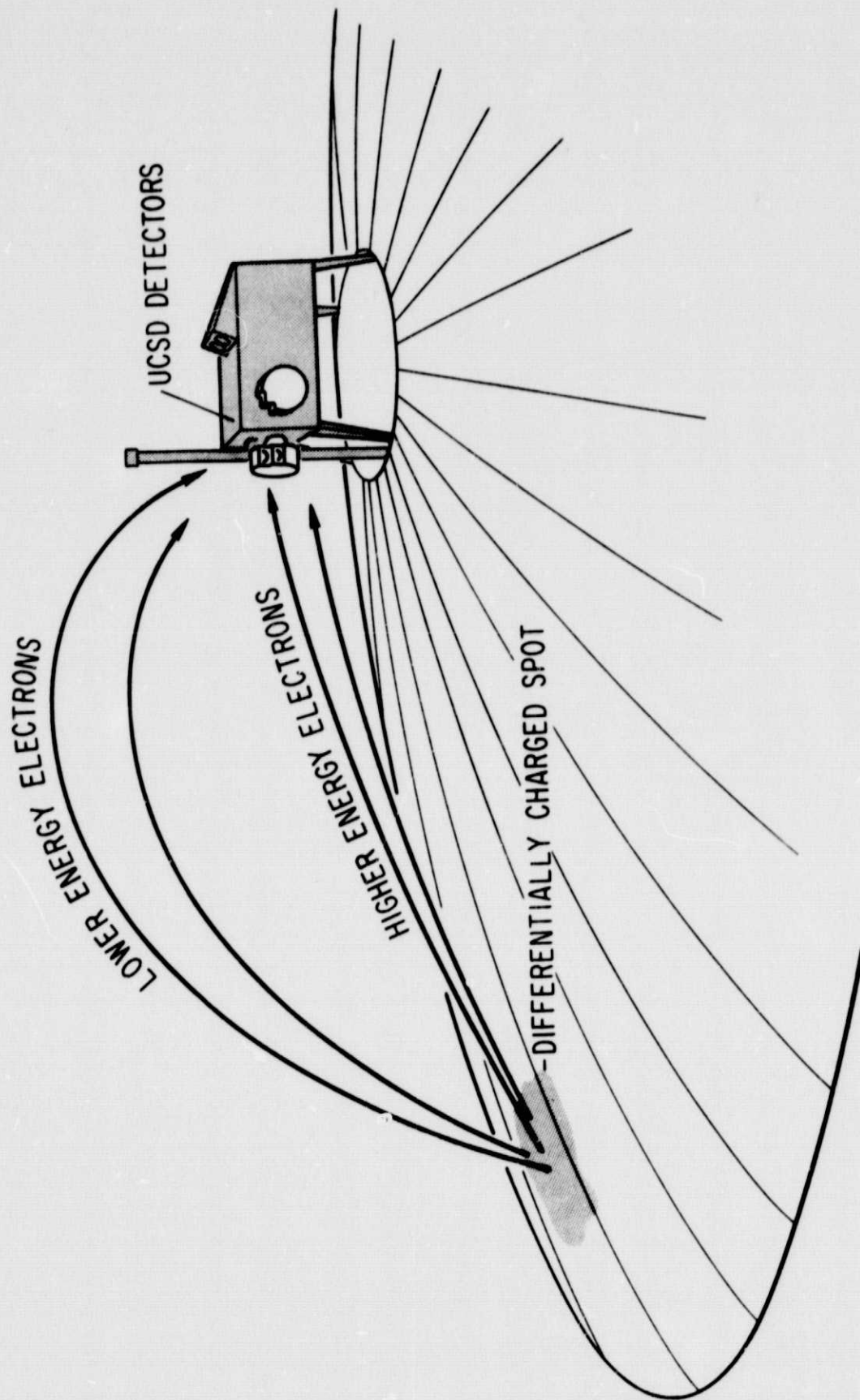


FIGURE 18

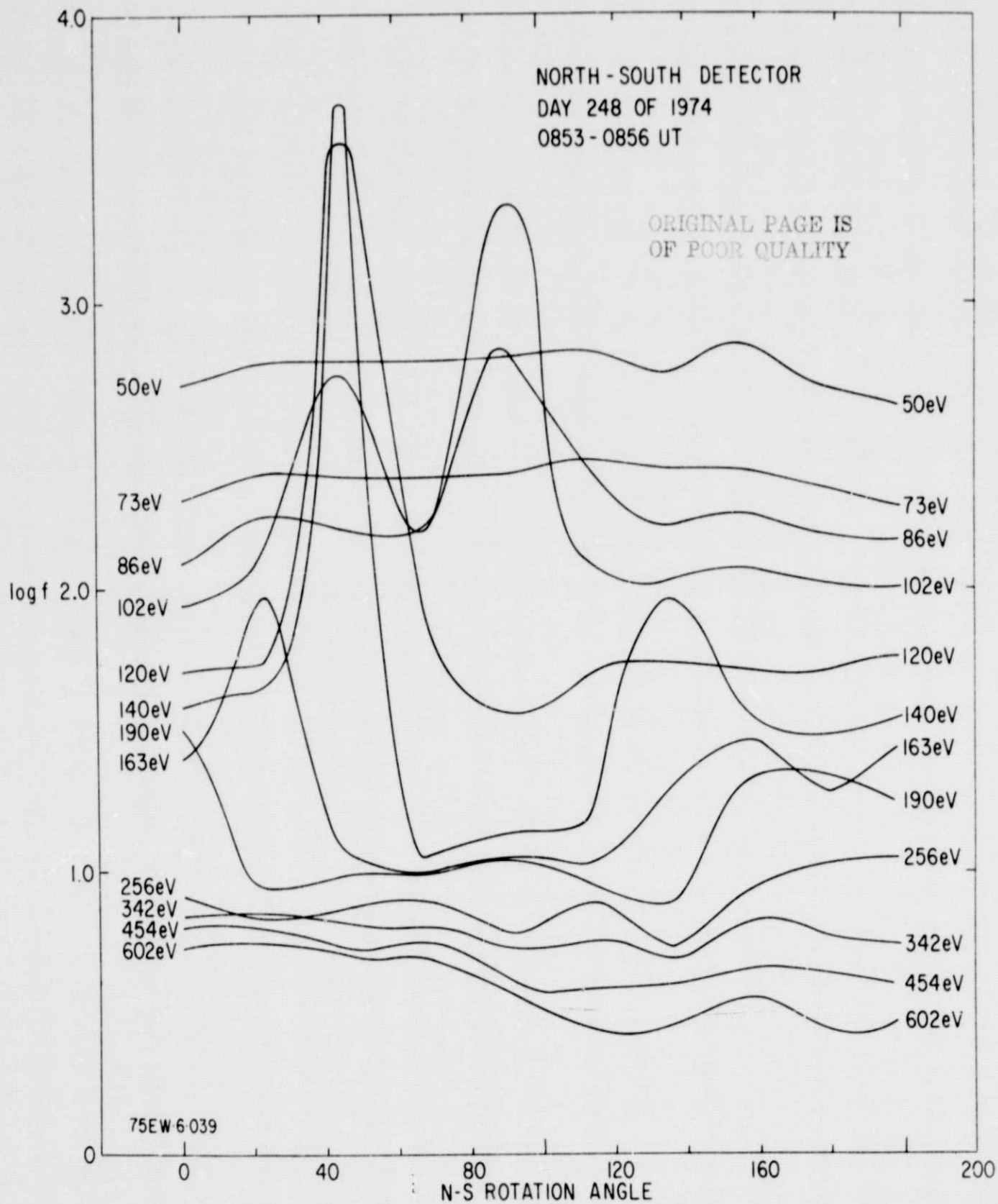


FIGURE 19

ORIGINAL PAGE IS
OF POOR QUALITY

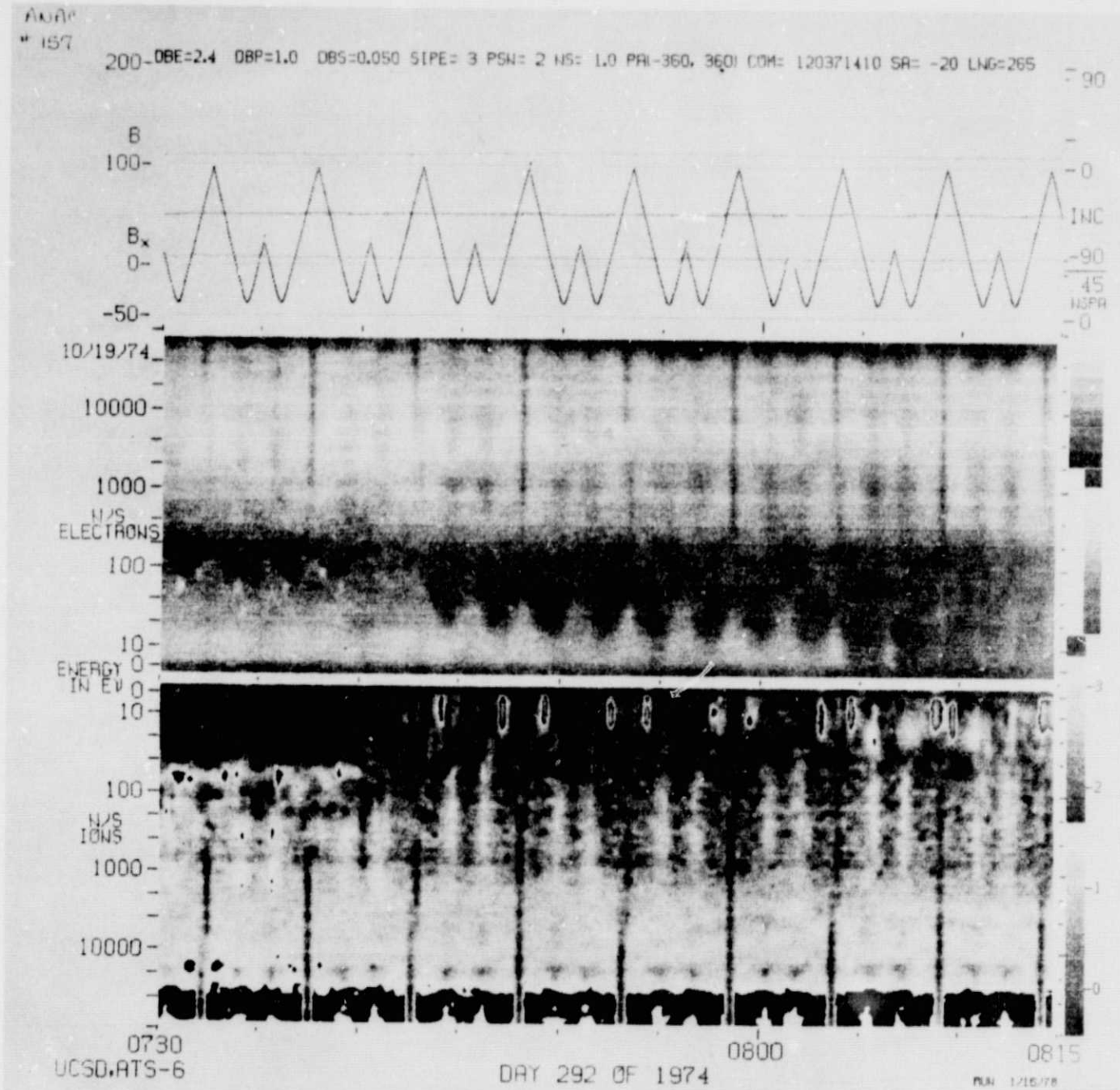


FIGURE 20